

An efficient algorithm to compute the minimum free energy of interacting nucleic acid strands

Ahmed Shalaby*

Damien Woods*

Abstract

The information-encoding molecules RNA and DNA form a combinatorially large set of secondary structures through nucleic acid base pairing. Thermodynamic prediction algorithms predict favoured, or minimum free energy (MFE), secondary structures, and can even assign an equilibrium probability to any particular structure via the partition function—a Boltzmann-weighted sum of the free energies of the exponentially large set of secondary structures. Prediction is NP-hard in the presence pseudoknots—base pairings that violate a restricted planarity condition. However, unspseudoknotted structures are amenable to dynamic programming-style problem decomposition: for a single DNA/RNA strand there are polynomial time algorithms for MFE and partition function. For multiple strands, the problem is significantly more complicated due to extra entropic penalties. Dirks et al [SICOMP Review; 2007] showed that for multiple ($\mathcal{O}(1)$) strands, with N bases, there is a polynomial time in N partition function algorithm, however their technique did not generalise to MFE which they left open.

We give the first polynomial time ($\mathcal{O}(N^4)$) algorithm for unspseudoknotted multiple ($\mathcal{O}(1)$) strand MFE, answering the open problem from Dirks et al. The challenge in computing MFE lies in considering the rotational symmetry of secondary structures, a global feature not immediately amenable to dynamic programming algorithms that rely on local subproblem decomposition. Our proof has two main technical contributions: First, a polynomial upper bound on the number of symmetric secondary structures that need to be considered when computing the rotational symmetry penalty. Second, that bound is leveraged by a backtracking algorithm to find the true MFE in an exponential space of contenders.

Our MFE algorithm has the same asymptotic run time as Dirks et al’s partition function algorithm, suggesting a reasonably efficient handling of the global problem of rotational symmetry, although ours has higher space complexity. Finally, our algorithm also seems reasonably tight in terms of number of strands since Codon, Hajiaghayi and Thachuk [DNA27, 2021] have shown that unspseudoknotted MFE is NP-hard for $\mathcal{O}(N)$ strands.

1 Introduction

The *primary structure* of a DNA strand is simply a word over the alphabet $\{A, C, G, T\}$, or $\{A, C, G, U\}$ for RNA. Bases may bond in pairs, A binds to T and C binds to G, and a set of such pairings for a strand is called a *secondary structure* as shown in Figure 1(a); typically each strand has exponentially many possible secondary structures.¹ Mainly, what practitioners care

*Hamilton Institute and Department of Computer Science, Maynooth University, Ireland. Research supported by Science Foundation Ireland (SFI) under grant numbers 20/FFP-P/8843 and 18/ERC/5746 and the European Union’s European Research Council (ERC, Active-DNA, no 772766); European Innovation Council (EIC, DISCO, No 101115422). Views and opinions expressed are however those of the author(s) only and do not necessarily reflect those of the European Union, European Research Council, European Innovation Council or Science Foundation Ireland. Neither the European Union nor the granting authority can be held responsible for them.

¹A secondary structure, along with a set of experimental conditions, induces one or more 3D structures called tertiary structures—a complication we will not be concerned with in this paper since, unlike proteins, it is fortunate that DNA/RNA interactions are sufficiently chemically simple that that somewhat elementary secondary structure model is sufficient for useful structural prediction.

| Input type | MFE | Partition function |
|---|---|--|
| Single strand | $\mathcal{O}(N^4)$ [49, 48, 27, 26, 41] | $\mathcal{O}(N^4)$ [24] |
| Multiple strands, bounded, i.e. $c = \mathcal{O}(1)$ strands | $\mathcal{O}(N^4(c-1)!)$ [Theorem 1] | $\mathcal{O}(N^4(c-1)!)$ [10] ⁵ |
| Multiple strands, unbounded, i.e. $\mathcal{O}(N)$ strands | APX-hard [9] | Open problem |

Table 1: Some algorithmic results for MFE and partition function for unpsudoknotted² nucleic acid systems. N is the total number of bases of all strand(s) in the system (i.e. sum of strand lengths). Results are shown for input being a single strand, multiple strands bounded by a constant or unbounded/growing with N . Note that in the literature the polynomial is sometimes written to the power 3 (e.g. $\mathcal{O}(N^3\dots)$), but this is for a restricted “relaxation” of the model.⁵

about are probabilities of a given secondary structure or class of secondary structures. For that, each secondary structure s has an associated, typically negative, real valued *free energy* $\Delta G(s)$, where more negative is deemed more favourable. Thus the most favourable is the secondary structure, or structures, with minimum free energy (MFE). More generally, the Boltzman distribution is a probability distribution on secondary structures s at chemical equilibrium: the probability of s is $p(s) = \frac{1}{Z}e^{-\Delta G(s)/k_B T}$ where Z is a normalisation factor called the partition function:

$$Z = \sum_{s \in \Omega} e^{-\Delta G(s)/k_B T} \quad (1)$$

that is, an exponentially weighted sum of the free energies over the set Ω of all secondary structures, where k_B is Boltzmann’s constant and T is temperature in Kelvin.

Decades ago, the deep relationship between secondary structures and dynamic programming algorithms was established [49, 48, 27, 26, 41, 24]. If a secondary structure can be drawn as a polymer graph without edge crossings it is called unpsudoknotted (Figure 1(c)). The earliest polynomial time algorithms were for single-stranded unpsudoknotted secondary structures, with the absence of crossings allowing for planar decompositions of secondary structures that are suited to dynamic programming techniques.² For a single RNA/DNA strand, both MFE and partition function are computable in $\mathcal{O}(N^4)$ time (Table 1), using the standard energy model³ that will be formally defined in Section 2.

Work in DNA computing [44, 28, 36, 39, 14, 6, 34, 46], and nucleic acid nanotechnology more generally [16, 43], involves building molecular systems and structures with, to date, hundreds, and soon, thousands, of interacting strands, so there is a need for better algorithms for these multi-stranded ‘inverse design problems’ [8, 13]. And, of course, biologists need to understand molecular structure in order to understand and predict molecular interactions. However, when there are multiple interacting strands, the situation becomes significantly more complicated than

²Exclusion of pseudoknots is usually founded on both modelling and algorithmic considerations. Energy models for pseudoknots are difficult to formulate due to the increased significance of geometric issues and tertiary interactions [10]. If pseudoknots are permitted, it is known that the MFE prediction is NP-hard even for a single strand [1, 20, 21]. The first NP-hardness results [1, 20] used a simple energy model called the stacking model where only consecutive base pairs forming a stack contribute to the free energy of a secondary structure. These hardness results with relatively simple energy models, make it seem unlikely that the MFE prediction problem will be easier in the case of more complicated energy models [9]. But, dynamic programming algorithms are still possible for restricted classes of pseudoknots, for both MFE prediction [30, 38, 7, 18, 29] and partition function [11, 12].

³This model is variably called the nearest neighbour model, the Turner model, and loop energy model. Versions of the model have been implemented in software suites such as NUPACK [10, 12, 15], ViennaRNA [19] and mfold [47], for both RNA and DNA [31, 32].

the single-stranded case for two reasons: First, for a secondary structure to be unpsuedoknotted, it implies there should be *at least one* permutation of the strands without crossings on the polymer graph [10] (Figure 1). Second, if strand types are repeated then so-called *rotational symmetries* (Figure 2) arise that need to be accounted for in the model to match the underlying statistical mechanics⁴, otherwise structures may be over- or undercounted, leading to incorrect probabilities in the Boltzmann distribution, in other words: incorrect predicted free energy of a secondary structure.

For multiple strands, albeit a constant number $c = \mathcal{O}(1)$, Dirks, Bois, Schaeffer, Winfree and Pierce [10] gave a polynomial time partition function algorithm running in time $\mathcal{O}(N^4(c-1)!)$.⁵ The first problem goes away by simply assuming c is a constant; but if the number of strands is non-constant, in particular $c = \mathcal{O}(N)$, Codon, Hajiaghayi and Thachuk [9] showed MFE is NP-hard, and even APX-hard.⁶ For the second, rotational symmetry, problem, in order to compute partition function, Dirks et al [10] found an algebraic link between the overcounting and the rotational symmetry correction problems, which allowed both to be solved simultaneously, aided by the exponential nature of the partition function. Surprisingly, that trick does not work for MFE: Since MFE prediction is minimization-based, there is no secondary structure overcounting problem in MFE prediction—repeated secondary structures will not change the outcome of minimization, unlike the partition function which is summation-based. Hence, the absence of the overcounting problem makes MFE prediction harder to solve, and was left open by Dirks et al [10]. For the special case of two strands, Hofacker, Reidys, and Stadler [17] gave an $\mathcal{O}(N^6)$ algorithm. In this paper, we propose an efficient solution to the $\mathcal{O}(1)$ strand MFE problem, the first that runs in polynomial time.

1.1 Statement of main result

Our main result is the following theorem, whose proof is in Section 5:

Theorem 1. *There is an $\mathcal{O}(N^4(c-1)!)$ time and $\mathcal{O}(N^4)$ space algorithm for the Minimum Free Energy unpsuedoknotted secondary structure prediction problem, including rotational symmetry, for a set of $c = \mathcal{O}(1)$ DNA or RNA strands of total length N bases.*

In Section 5 we give a time-space trade-off for our result, by showing a variation of the algorithm runs in $\mathcal{O}(N^4 \log N(c-1)!)$ time but $\mathcal{O}(N^3)$ space.

We use the standard [10] definition of free energy (Eq. (2)) of multistranded unpsuedoknotted secondary structures, which includes rotational symmetry, see Section 2 for formal definitions. We first give an extensive overview of the proof and paper structure, followed by future work.

⁴This fact from statistical mechanics is discussed in some papers [10, 17], although we’ve not found its full derivation in the modern nucleic-acid algorithmic literature. We leave a first-principles derivation for future work.

⁵We note that Dirks et al [10], and others in field [49, 48, 9, 41, 24, 3], often state the run time with 3 instead of 4 in the exponent (i.e. $\mathcal{O}(N^3)$ for single stranded and $\mathcal{O}(N^3(c-1)!)$ for multistranded). This reduction comes from changing the standard energy model by putting some restrictions on the size of interior loops (Figure 1), or by enforcing certain mild conditions on the energy parameters for the interior loops [22, 17], we do not assume these additional assumptions in this work. Note that our time/space complexity could benefit from such model changes for example, via reduction of the upper bound in Lemma 23

⁶This hardness result holds whether or not rotational symmetries are accounted for in the energy model.

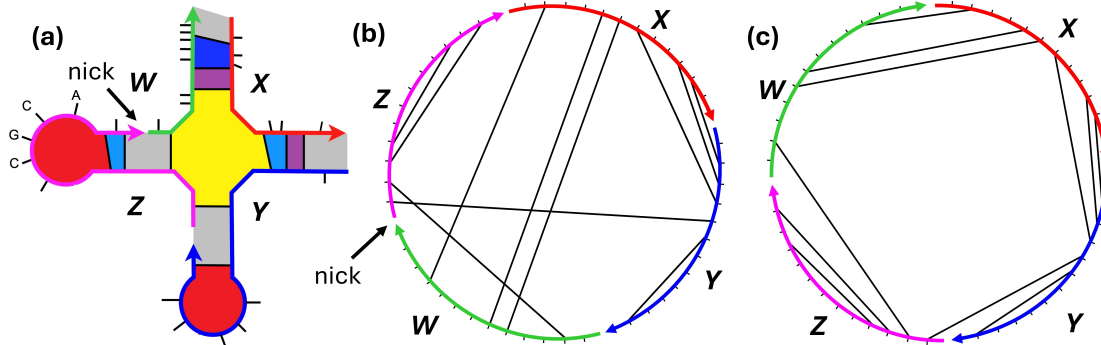


Figure 1: A DNA (or RNA) secondary structure S with $c = 4$ strands and two of its $(c-1)! = 6$ polymer graphs. (a) One of the many possible secondary structures for four DNA strands W, X, Y, Z . Short black lines represent DNA bases (a few are shown $\dots C, G, C, A \dots$), and long lines represent base pairs (drawing not to scale). Loops are colour-coded as follows: stack=purple, multiloop=yellow, hairpin=red, bulge=light blue, internal=dark blue, external=grey. Black arrow: the small gap between two strands is called a *nick*. (b) Polymer graph for the strand ordering $\pi' = WZXY$, denoted $\text{Poly}(S, \pi')$, showing base-pair crossings. (c) By reordering to $\pi = WXYZ$ we get another polymer graph $\text{Poly}(S, \pi)$ for S , without crossings, hence S is unpsuedoknotted.

1.2 Proof overview and paper structure

1.2.1 The main challenge: handling rotational symmetry

Typically, each DNA base pair that forms represent a decrease (improvement in favourability) in free energy—although not always. In a multi-stranded system, when several strands bind together the entropy of the overall system is decreased since there are now less states due to their being less free molecules. Thus the energy model for multistranded systems includes an entropic *association penalty* (typically positive) for every extra strand, beyond the first, bound into a multistranded molecular complex [10]. However, statistical mechanics tells us to be careful about symmetry: with multiple identical strands in a complex it is possible that the complex is rotationally symmetric, intuitively there are several complexes, identical up to rotation of their polymer graphs (Figure 2).⁷ These so-called indistinguishable complexes, in turn imply that a (positive) penalty should be applied to account for the difference in entropy between a similar, but distinguishable, complex without rotational symmetry [4, 2, 35, 15].⁴ Section 2 gives definitions needed to formalise these concepts, including: DNA, unpsuedoknotted secondary structure, polymer graph, free energy including rotational symmetry (Eq. (2)) and MFE (Eq. (3)). In particular, Section 2.3 gives a group-theoretic definition of rotational symmetry, to help formalise some of the prior work.

1.2.2 General approach to find the true MFE

One obvious idea might be to find a dynamic programming algorithm that directly handles rotational symmetry. However, this approach suffers from rotational symmetry being a *global property* of an entire system state (secondary structure), whereas dynamic programming relies on piecing together subproblems that are individually unaware of the global context—or more precisely, may be used in multiple global contexts whether symmetric or not.

Instead, our strategy is to first compute what we call the *symmetry-naive MFE* (snMFE) that

⁷Formally, we mean the permutation representing the complex is rotationally symmetric.

(incorrectly) assumes all strands are distinct and thus does not compute correct free energies for rotational symmetries. We use Dirks et al’s snMFE algorithm [10], that assumes all strands are distinct, but augmented to return extra dynamic programming matrices (Algorithm 1 in Appendix B). We use these extra matrices to compute the required symmetry correction to that snMFE value using a backtracking algorithm, as follows.

1.2.3 Polynomial upper bound: intuition for Section 3

Our goal is to show that, after running our augmentation of the known algorithm for snMFE, we have implicit access to a collection of secondary structures that are ‘not too far’ from the true MFE—where by ‘not too far’ we mean we have a polynomial bound on the number of structures to be considered by another fast (“backtracking”) algorithm that finds the true MFE structure.

First, to see how we find this polynomial bound, imagine the augmented snMFE algorithm finds that the secondary structure with snMFE is rotationally *asymmetric*, hence we are done, we know that the snMFE value is in fact the true MFE. Otherwise, we have a *rotationally symmetric* secondary structure: ideally we would like to compute it’s rotational symmetry degree R (takes linear time in the size of the secondary structure) and then return $\text{snMFE} + k_B T \log R$ as the true MFE, but this approach is doomed to fail since there could also be structures with lower true MFE, i.e. in the real interval $[\text{snMFE}, \text{snMFE} + k_B T \log R) \subset \mathbb{R}$.

Leveraging the two properties of being (a) unspseudoknotted and (b) rotationally symmetric, in Section 3 we define a class of cuts of a structure’s polymer graph (Figure 1) that we call *pizza cuts*, or, more formally, *admissible symmetric backbone cuts* (Definition 14). These cuts are radially symmetric, hence the name pizza cut—how one slices a pizza from disk-edge to centre. In Lemmas 13 and 22, we show that there are at most a polynomial number of pizza cuts that symmetric structures may have.

Then, when we do a backtracking-based search (below), through the dynamic programming matrices from the structure(s) with snMFE, to larger free energies: if we find two different symmetric pizzas, but with the same pizza cuts, we make a new pizza, by swapping a slice from one with a slice from the other. We prove that the new pizza is (a) guaranteed to be asymmetric and (b) has free energy sandwiched between the snMFE values of two symmetric structures (Lemmas 20 and 22). Moreover, this new structure’s free energy is the true MFE. Otherwise we either find a symmetric structure (we output its naive free energy as the true MFE), or we reach a contradiction (i.e. which can not happen) by reaching the polynomial bound having exhausted the set of all *admissible symmetric backbone cuts*. In all cases the true MFE and its structure are output.

1.2.4 Backtracking to find the true MFE: intuition for Section 4

It remains to show how we will do the backtracking search mentioned above. In Section 4 we analyse the backtracking algorithm, which is given in Algorithm 2 in Appendix C, and is a polynomial time algorithm over the exponentially large set of structures ‘close’ to the true MFE value. It scans all secondary structures within an energy level starting with the symmetry-naive MFE (snMFE) energy level, it goes on to sequentially scan higher levels in low-to-high order. The scanning process at any energy level \mathcal{E} guarantees that each secondary structure that belongs to \mathcal{E} should be scanned exactly once.

The backtracking algorithm will run until one of the following conditions occurs: (1) It scans an asymmetric secondary structure S , or (2) it exceeds the polynomial upper bound \mathcal{U} of the number of symmetric secondary structures (i.e. the number of distinct pizza cuts) to be scanned, or (3) the backtracking will start scanning a new energy level $\mathcal{E}' > \mathcal{B}$, where \mathcal{B} is the current best candidate

for MFE (the starting value for \mathcal{B} is $\mathcal{B} = \text{snMFE} + k_B \log v(\pi)$ where $v(\pi)$ is the highest degree of rotational symmetry, Definition 9). Then, based on the condition that will occur, the algorithm directly returns the true MFE, and a secondary structure which has the true MFE will also be constructed. The short proof of Theorem 1 in Section 5 ties these results together to give the final analysis of our main result.

1.3 Future work

Our algorithm runs in polynomial time $\mathcal{O}(N^4(c-1)!)$ for the case of $c = \mathcal{O}(1)$ strands, the $(c-1)!$ term coming from the fact that our algorithm, as well as Dirks et al [10], is assumed to be called from an outer loop that explicitly tries all $(c-1)!$ cyclic strand permutations. Can we increase the number of strands and still have a polynomial time algorithm? We know “not by much”, since the problem is NP-complete when $c = \mathcal{O}(N)$ [9]. Interestingly, Boehmer, Berkemer, Will, and Ponty [3] recently reduced the c -strand parameterized running time for computing symmetry-naive MFE (i.e. ignoring rotational symmetry) and partition function from factorial, $\mathcal{O}(N^4(c-1)!)$, to exponential, $\mathcal{O}(N^4 3^c)$.⁵ It is feasible that our MFE algorithm could be augmented via this result.

Our MFE algorithm exploits a polynomial upper bound, \mathcal{U} , on the number of so-called symmetric secondary structures, or distinct pizza cuts. That bound is linear in “most” cases (Lemma 24), but quadratic in one special subcase (Lemma 22) of 2-fold rotational symmetry with a central internal loop. Reducing that special case to linear would subtract one from our algorithm’s running time exponent.

Table 1 shows the open problem for partition function on multiple strands. Intuitively, it seems that partition function should be at least as hard as MFE, however that intuition is tempered by the fact that Dirks et al’s approach for partition function did not carry over to MFE, hence this is an open problem. Indeed, our paper brings extra techniques to handle multi-stranded MFE.

More generally, the computational complexity of partition function for DNA/RNA strands is less well understood than MFE. For example, are there settings where partition function, or problems counting numbers of structures, are #P-complete?

2 Definition of multi-stranded DNA systems and basic lemmas

Intuitively, a single DNA strand s is a sequence of nucleotide bases connected by covalent bonds which together make up the backbone of s , with the left end of the sequence corresponding to the 5’ end of s and the right end corresponding to the 3’ end. When drawing s we label the 3’ end with an arrow which also shows the strand directionality, see Figure 1. Hydrogen bonds can form between Watson-Crick base pairs, namely C–G and A–T.

Formally, A DNA strand s is a word over the alphabet of DNA *bases* $\{A, T, G, C\}$, indexed from 1 to $|s|$, where $|s|$ denotes the length of s . A base pair is a tuple (i, j) such that $i < j$. For any c strands, we will assign to each of them a unique distinct identifier in $\{1, \dots, c\}$ [10]. Each base is specified by a strand identifier and a position on that strand, i_s denotes the base of index i of strand s .

2.1 Connected unpseudoknotted secondary structures and polymer graphs

Definition 2 (Secondary structure S). For any set of c DNA strands, a secondary structure S is a set of base pairs such that each base appears in at most one pair, i.e. if $(i_n, j_m) \in S$ and $(k_q, l_r) \in S$ then i_n, j_m, k_q, l_r are all distinct.

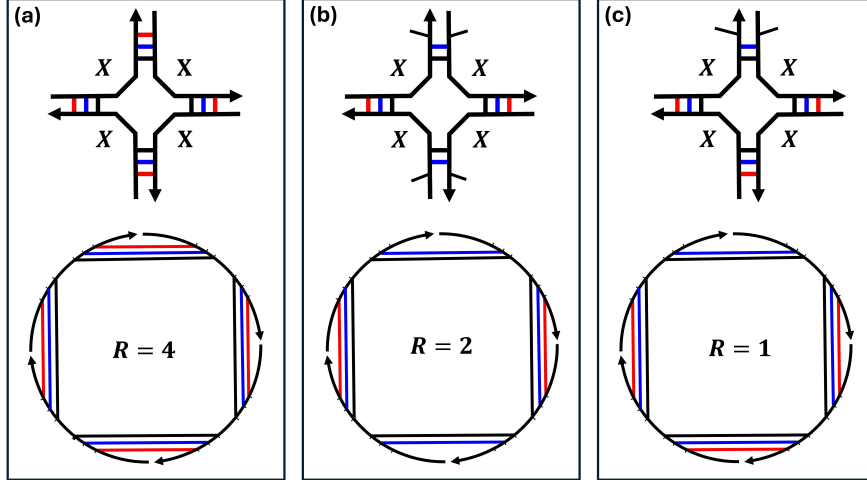


Figure 2: Three secondary structures with their associated polymer graphs. In each case, there is a single complex with four identical (indistinguishable) strands of strands of type X , but with different symmetry degree R . (a) Symmetry degree $R = 4$ (rotation by 90° gives the same secondary structure). (b) Symmetry degree $R = 2$ (rotation by 180° gives the same secondary structure). (c) Symmetry degree $R = 1$ (asymmetric secondary structure).

The *graph representation of a secondary structure* S is the graph $G = (V, E)$, where V is the set of bases of each strand $s \in \{1, \dots, c\}$, and $E = E_v \cup E_b$, where E_v is the set of *covalent backbone bonds* connecting base i_n with base $(i + 1)_n$ for all bases $i = 1, 2, \dots, |n| - 1$ on all strands $n \in \{1, \dots, c\}$, and $E_b = S$ is the set of base pairs in S . E_v and E_b are disjoint.

The set of circular permutations, Π , of c strands has $(c - 1)!$ distinct circular permutations [5] (e.g., for the three strands $\{A, B, C\}$, $\Pi = \{ABC, ACB\}$), e.g., the orderings ABC , BCA , and CAB are the same on a circle. Next, we define a polymer graph for each π , see also Figure 1.

Definition 3 (Polymer graph). For any secondary structure S , and any ordering π of its c strands, the polymer graph representation of S , denoted $\text{Poly}(S, \pi)$, is a graph representation of S , embedded in the unit disk from \mathbb{R}^2 , where the c strands are placed in succession from their 5' to 3' ends around the circumference of the circle, and the bases, V , are spaced evenly around the circle circumference, each element of E_v is represented by an arc on the circumference between covalently-bonded bases, and each element of E_b is represented by a chord between two different bases.

Definition 4 (Unpseudoknotted secondary structure). A secondary structure S is unpseudoknotted if there exists at least one circular permutation $\pi \in \Pi$ such that $\text{Poly}(S, \pi)$ is planar, otherwise S is pseudoknotted. An example is shown in Figure 1.

Remark 5. In the rest of the paper we use N to denote the total number of bases of a secondary structure S . A secondary structure S is connected if the graph representation of S is a connected graph. In this work, we are only interested in connected unpseudoknotted secondary structures.

2.2 Free energy of a secondary structure

Any connected unpseudoknotted secondary structure S can be decomposed into different loop types [37, 32, 23]: namely hairpin loops, interior loops, exterior loops, stacks, bulges, and multiloops

as shown in Figure 1. As usual, let k_B be Boltzmann’s constant and T is the temperature in Kelvin (also a constant).⁸ The free energy of S is defined as the sum of three terms:⁹

$$\Delta G(S) = \sum_{l \in S} \Delta G(l) + (c - 1)\Delta G^{\text{assoc}} + k_B T \log R. \quad (2)$$

- the first is itself the sum of the (well-defined, empirically-obtained) free energies $\Delta G(l)$ of S ’s constituent loops [10], where each loop energy is defined with respect to the free energy of the unpaired reference state.
- ΔG^{assoc} is the entropic association [10] penalty applied for each of the $c - 1$ strands added to the first strand to form a complex of c strands.
- R is the rotational symmetry of the secondary structure S , illustrated in Figure 2, and to be formally defined in Section 2.3. In particular, since favourable free energies are usually negative, the term $k_B T \log R \geq 0$ corresponds to the reduction in the entropic contribution of S , as any secondary structure with an R -fold rotational symmetry has a corresponding R -fold reduction in its distinguishable conformational space [10] as shown in Figure 2.¹⁰ Dynamic programming algorithms to date for multi-stranded MFE ignored this term for reasons we outline in Section 2.3.

For c strands, we let Ω be the set (usually called the *ensemble*) of all connected unpseudo-knotted secondary structures. For any circular permutation $\pi \in \Pi$ of the c strands, let $\Omega(\pi) \subseteq \Omega$ be the subset of Ω such that each connected unpseudo-knotted secondary structure $S \in \Omega(\pi)$ is representable as a crossing-free polymer graph with circular permutation π .

Remark 6 (S , or $\text{Poly}(S, \pi)$). Dirks et al. [10] showed, in their representation theorem (Theorem 2.1), that the sets $\Omega(\pi)$, for all $\pi \in \Pi$, form a partitioning of Ω , which means that every connected unpseudo-knotted secondary structure belongs to exactly one $\Omega(\pi)$ for some $\pi \in \Pi$. Hence to avoid the cumbersome phrase *c-strand connected unpseudo-knotted secondary structure S with strand ordering π and polymer graph $\text{Poly}(S, \pi)$* we simply write S , or $\text{Poly}(S, \pi)$.

Predicting the minimum free energy means finding a minimum over the ensemble Ω . The known strategy is to deal with each partition $\Omega(\pi)$ separately, then finding their minimum:

$$\text{MFE} = \min_{S \in \Omega} \Delta G(S) = \min_{\pi \in \Pi} \left\{ \min_{S \in \Omega(\pi)} \Delta G(S) \right\} \quad (3)$$

2.3 Definition of multi-stranded rotational symmetry

Here, we formalise rotational symmetry. In the previous section we assigned each one of the c strands a unique identifier, dealing with them as distinct strands even if two or more have the same sequence. But in most experimental settings, strands with the same sequences are *indistinguishable* in the sense that they behave identically with respect to relevant measurable quantities [10]. Mathematically, we say that *two strands are indistinguishable* if they have the same sequence. Also, *two secondary structures are indistinguishable* if there exists a permutation of the implied unique

⁸All results hold if we assume these are typical values from physics, or just 1 in appropriate units.

⁹Throughout this paper $\log n = \log_e n$.

¹⁰This is perhaps counter-intuitive. In a follow-up expanded version of this paper we will give a full statistical mechanics explanation, which treats the symmetry penalty to offset the fact that non-symmetrical structures are undercounted.

strand ordering (Remark 6), that maps indistinguishable strands onto each other while preserving all base pairs, otherwise, the two structures are distinct [10].

For any c strands, not necessarily distinct, they consist of $k \leq c$ *strand types*, usually denoted by uppercase English letters X, Y, \dots .¹¹ A *multi-stranded DNA system* $M = \{(t_1, n_1), (t_2, n_2), \dots, (t_k, n_k)\}$, is a *multiset* of k strand types t_1, \dots, t_k with repetition numbers $n_1, \dots, n_k \in \mathbb{N}$ such that $n_1 + \dots + n_k = c$.¹² For such a multiset M we can think of each circular permutation π as a string over strand types such that each strand type t_i appears exactly n_i times (e.g., $M = \{(X, 6), (Z, 3)\}$ one valid π is $\pi = XZXXZXZXZX$).

Definition 7 (Symmetry degree of a permutation). For any circular permutation π , we say $n \in \mathbb{N}$ is a symmetry degree of π if $\pi = y^n$ for some y , a prefix of π .

For example, $\{1, 2, 4\}$ are the symmetry degrees of $\pi = XZXXZXZXZX$ since $\pi = (XZXXZXZXZX)^1 = (XZXXZ)^2 = (XZ)^4$.

For any circular permutation π , its maximum symmetry degree is denoted $v(\pi)$, and the corresponding repeating prefix x , such that $x^{v(\pi)} = \pi$, is the *fundamental component* of π . It can be seen that x is the smallest prefix that repeats over π . Indeed, $v(\pi)$ is the number of cyclic permutations that map each strand to a strand of the same type. Any repeating prefix of π must be a multiple of its fundamental component, as proven in Lemma 33 in Appendix A.

Remark 8 (Notation: X_m^n). For any circular permutation π , its *augmented version* gives the full ordering information for each fundamental component. For example, if $\pi = XYXZXYXZ$, then its fundamental component is $XYXZ$ and its augmented version is $X_1^1 Y_1^1 X_2^1 Z_1^1 X_1^2 Y_1^2 X_2^2 Z_1^2$, such that X_m^n , means the m th strand of type X in the n th fundamental component of π .

We can visualize any ordering π by representing it as a *regular $v(\pi)$ -gon* with each of its $v(\pi)$ vertices representing a fundamental component. Let $\rho = (1\ 2\ 3\ \dots\ v(\pi))$ ¹³ and consider the cyclic group¹⁴ G^π generated by ρ . Intuitively, G^π is the group of the all $v(\pi)$ rotational motions in plane of the regular $v(\pi)$ -gon that give the same $v(\pi)$ -gon. We can represent G^π as follows: $G^\pi = \{\rho^0, \rho^1, \dots, \rho^{v(\pi)-1}\}$, where ρ^i represents rotation of the regular $v(\pi)$ -gon by the angle of $i \times \frac{360^\circ}{v(\pi)}$, where $|G^\pi| = v(\pi)$.

Now, we are ready to define the rotational symmetry of a secondary structure and a strand ordering π , intuitively, the number of rotations of its polymer graph that give the same polymer graph, as shown in Figure 2.

Definition 9 (R -fold rotational symmetric structure). A connected unpsuedoknotted secondary structure S and strand ordering π (and thus polymer graph $\text{Poly}(S, \pi)$) is R -fold rotational symmetric, or simply rotationally symmetric, then for any base pair (i, j) in the polymer graph $\text{Poly}(S, \pi)$ the rotation of that base pair by multiples of $(360^\circ/R)$ is also in $\text{Poly}(S, \pi)$. More formally: $(i_{X_k^l}, j_{Y_m^n}) \in \text{Poly}(S, \pi)$, iff $(i_{X_k^{a(l)}}, j_{Y_m^{a(n)}}) \in \text{Poly}(S, \pi)$ for all $a \in H \leq G^\pi$, where H is the largest subgroup¹⁵ satisfying the condition, and if $|H| = R$.

¹¹In contrast with some of the literature. we exclude using $\{A, T, G, C\}$ for strand types; to avoid any confusion between strand and base types.

¹²It is known [33] how to efficiently reduce the circular permutation space by getting rid of circular permutations that are redundant due to indistinguishable strands, which is important to consider when computing the partition function but needed for MFE.

¹³Here we use algebraic cycle notation. The order of ρ , denoted by $o(\rho)$, is the length of ρ which is $v(\pi)$.

¹⁴ G^π is isomorphic to $C_{v(\pi)}$, cyclic group of order $v(\pi)$.

¹⁵ $H \leq G$, notationally means H is a subgroup of G . Every subgroup of cyclic group is also cyclic.

Remark 10. In Def. 9, we restricted H to be the *largest* subgroup so as to be aligned with the entropic reduction penalty due to symmetry that appears in Eq. (2), even if from a geometric perspective any R -fold rotational symmetric secondary structure should be also R' -fold rotational symmetric if R' divides R .

3 A polynomial upper bound on a class of rotationally symmetric secondary structures

Remark 11. In this section, we assume a global indexing of all bases from 1 to N , and use square brackets, $[i, i + 1]$, to denote the covalent bond connecting bases i and $i + 1$, given that both belong to the same strand. This notation also helps to differentiate covalent bonds $[i, i + 1]$ from base pair (j, k) (hydrogen bonds) notation.

Definition 12 (R -symmetric backbone cut generated by a covalent bond). For a connected unpseudoknotted secondary structure S and strand ordering π , the R -symmetric backbone cut generated by the covalent bond $b = [i_{A_m^n}, (i + 1)_{A_m^n}]$ is $\mathcal{C}_R^b = \{[i_{A_m^{a(n)}}, (i + 1)_{A_m^{a(n)}}] : \text{for all } a \in H \leq G^\pi \text{ such that } |H| = R\}$. We call b a *symmetric backbone cut generator*. An example is shown in Figure 3.

Only one covalent bond is needed to generate its corresponding R -symmetric backbone cut. Also, note that this definition excludes any cut through nicks by Remark 11. The next lemma shows that the number of unique symmetric backbone cuts is linear in N .

3.1 Linear upper bound on number of unique symmetric backbone cuts

Lemma 13 (Upper bound on unique symmetric backbone cuts). *For any connected unpseudoknotted secondary structure S of $c = \mathcal{O}(1)$ strands with N total bases, with a specific strand ordering π , the number of unique symmetric backbone cuts is $\frac{N-c}{v(\pi)} [\sigma(v(\pi)) - v(\pi)] = \mathcal{O}(N)$, where $\sigma(v(\pi))$ is sum of divisors of $v(\pi)$.*

Proof. In general, any covalent bond is a potential candidate for a symmetric backbone cut generator. For secondary structure S with N bases and c strands, there are $N - c$ covalent bonds in S by excluding all nicks. We need to compute the total number of all possible symmetric backbone cuts for every possible symmetry degree R . Given a specific R , the number of R -symmetric backbone cuts is $\frac{N-c}{R}$, since for any covalent bond x in a cut \mathcal{C}_R^b , we have $\mathcal{C}_R^x = \mathcal{C}_R^b$ (all bonds in that cut generate the same cut). And, hence for any two covalent bonds x and y , either $\mathcal{C}_R^x = \mathcal{C}_R^y$ or they are disjoint.

Because of symmetry (see Lemma 34), $R > 1$ and R divides $v(\pi)$ (denoted $(R \neq 1)|v(\pi)$ below). Assume that $d_1, d_2, \dots, v(\pi)$ are divisors of $v(\pi)$ such that $d_i \neq 1$, and since divisors happen in pairs

($d_i d'_i = v(\pi)$), then the total number of symmetric backbone cuts is

$$\begin{aligned}
\sum_{(R \neq 1) | v(\pi)} \frac{N - c}{R} &= (N - c) \sum_{(R \neq 1) | v(\pi)} \frac{1}{R} \\
&= (N - c) \left[\frac{1}{d_1} + \frac{1}{d_2} + \dots + \frac{1}{v(\pi)} \right] \\
&= (N - c) \left[\frac{d'_1}{d_1 d'_1} + \frac{d'_2}{d_2 d'_2} + \dots + \frac{1}{v(\pi)} \right] \\
&= (N - c) \left[\frac{d'_1 + d'_2 + \dots + 1}{v(\pi)} \right] \\
&= \frac{N - c}{v(\pi)} [\sigma(v(\pi)) - v(\pi)]
\end{aligned}$$

which is $\mathcal{O}(N)$ since $|\pi| = c = \mathcal{O}(1)$ (i.e. number of strands $c = \mathcal{O}(1)$). \square

If S is a connected unpseudoknotted secondary structure with ordering π , you can go from any base i to j in two different paths around the circumference of $\text{Poly}(S, \pi)$ (clockwise or anticlockwise). We define the *length* function $l[i, j]$ to be the length of the shorter path, including both i and j as follows:

$$l[i, j] = \min\{|i - j| + 1, N - |i - j| + 1\} \quad (4)$$

Also, $\llbracket i, j \rrbracket$ is used to denote that shorter *segment* of length $l[i, j]$, where the direction from base i to base j is the same as the system strands' direction.

3.2 How to slice a pizza (secondary structure)

We want to slice any R -fold rotational symmetric secondary structure S , **like pizza**, to the centre of its $\text{Poly}(S, \pi)$, without intersecting any of its base pairs. First, we formalise (Definition 14) a special type of backbone cut, called an *admissible R -symmetric backbone cut*. Then, we will prove (Lemma 15) its existence for S .

Definition 14 (Admissible R -symmetric backbone cut). For any connected unpseudoknotted secondary structure S with strand ordering π , the *R -symmetric backbone cut* \mathcal{C}_R^b generated by b is *admissible*, if for all covalent bonds $x \in \mathcal{C}_R^b$, x is not “enclosed” by any base pair $(i, j) \in \text{Poly}(S, \pi)$, more formally: $x \not\subseteq \llbracket i, j \rrbracket$. An example is shown in Figure 3.

Lemma 15. *For any R -fold rotationally symmetric secondary structure S , there exists at least one admissible R -symmetric backbone cut of S .*

Proof. From $\text{Poly}(S, \pi)$, select a base pair (i, j) that has maximal length $l[i, j]$: at least one of $[i - 1, i]$ and $[j, j + 1]$ must be a covalent bond, otherwise if both were nick S would be disconnected (a contradiction). We claim that this covalent bond, which we denote $[a, a + 1]$, is an admissible R -symmetric backbone cut generator, otherwise there exists a base pair $(m, n) \in \text{Poly}(S, \pi)$ such that $[a, a + 1] \subseteq \llbracket m, n \rrbracket$, giving a contradiction by either: (a) $\llbracket m, n \rrbracket$ must contain $\llbracket i, j \rrbracket$ which contradicts the maximality of $l(i, j)$, or (b) (m, n) and (i, j) intersect forming a pseudoknot. All covalent bonds in $\mathcal{C}_R^{[a, a+1]}$ have the same situation because of R -fold symmetry of S , which implies that $\mathcal{C}_R^{[a, a+1]}$ is an admissible R -symmetric backbone cut of S . \square

Note that any R -fold rotationally symmetric secondary structure S can have more than one admissible R -symmetric cut. Before defining what we mean by a pizza slice (formally, symmetric slice in Definition 17), the following lemma is used to ensure such a slice is connected.

Lemma 16 (Pizza slicing lemma). *For any $R \geq 2$ and any R -fold rotational symmetric secondary structure S , let G be the graph obtained from $\text{Poly}(S, \pi)$ by removing the covalent bonds of admissible R -symmetric backbone cut \mathcal{C}_R^b generated by any covalent bond b , such that $G = (V(\text{Poly}(S, \pi)), E(\text{Poly}(S, \pi)) \setminus \mathcal{C}_R^b)$, then G is disconnected and consists exactly of R connected isomorphic components.*

Proof. Lemma 15 ensures the existence of at least one admissible R -symmetric backbone cut of S , assume it is generated by $b = [i_{A_m^n}, (i+1)_{A_m^n}]$, then by Definition 12: $\mathcal{C}_R^b = \{[i_{A_m^{a(n)}}, (i+1)_{A_m^{a(n)}}] : \forall a \in H \leq G^\pi, |H| = R\}$. For any two (recall, $R \geq 2$) “consecutive” covalent bonds in \mathcal{C}_R^b (formally: $b_k = [i_{A_m^{a^k(n)}}, (i+1)_{A_m^{a^k(n)}}]$ and $b_{k+1} = [i_{A_m^{a^{k+1}(n)}}, (i+1)_{A_m^{a^{k+1}(n)}}]$), we construct the “pizza slice” G_k to be the subgraph of $\text{Poly}(S, \pi)$ induced by all vertices (or bases) that belong to $I_k = \llbracket (i+1)_{A_m^{a^k(n)}}, i_{A_m^{a^{k+1}(n)}} \rrbracket$. Intuitively, G_k is the slice we get after cutting $\text{Poly}(S, \pi)$ at b_k and b_{k+1} . At the end we will have a sequence of subgraphs $\mathcal{G} = \{G_1, G_2, \dots, G_R\}$. Because of symmetry, all subgraphs in \mathcal{G} are isomorphic. We claim that each subgraph in \mathcal{G} is exactly one connected component, and $G = \bigcup_{k=1}^R G_k$.

For any G_k , first we will show that G_k is disconnected from any other G_l with $l \neq k$, which follows from two observations: From Lemma 35 we know that the length of $I_k < \frac{N}{R}$ and I_1, \dots, I_R are disjoint segments by construction (via symmetry R), hence G_k and G_l are not connected by a covalent bond. To see that there is no base pair (x, y) connecting G_k and G_l : assume for the sake of contradiction that such a base pair (x, y) exists in $\text{Poly}(S, \pi)$, then one of the two covalent bonds b_k or $b_{k+1} \subseteq \llbracket x, y \rrbracket$ (by the definition of b_k, b_{k+1} above), contradicting the fact that \mathcal{C}_R^b is an admissible backbone cut. Also, it follows directly that $G = \bigcup_{k=1}^R G_k$ from the definition of inducing subgraphs.

We next wish to show that each slice G_k is connected. First, there exists $d \geq 1$ such that G consists of dR connected components, because for each k , $G_k \in \mathcal{G}$ is isomorphic (so if G_k has $d \geq 1$ components then all $G_l \in \mathcal{G}$ do also). Next we will show $d = 1$. Since G is the graph obtained from the connected graph $\text{Poly}(S, \pi)$ by removing $|\mathcal{C}_R^b| = R$ covalent bonds, so there are only two cases: (a) if each of these R covalent bonds is a cut edge, or bridge [42], G will consist of $R + 1$ components, contradicting the fact that number of its components must be dR for some $d \geq 1$, so $d = 1$, implying that each subgraph in \mathcal{G} consists of exactly one component. (b) The only other case is that G has R components (since we’ve already shown that the R slices are not connected to each other), giving the lemma statement. \square

Definition 17 (Symmetric slice). From the construction in Lemma 16, each of the R isomorphic subgraphs (components) in \mathcal{G} is called a *symmetric slice* of $\text{Poly}(S, \pi)$, denoted by \triangleright^S . Also, the loop free energy of a symmetric slice is:

$$\Delta G(\triangleright^S) = \sum_{l \in \triangleright^S} \Delta G(l) \quad (5)$$

For any R -fold symmetric secondary structure S , the following lemma shows the existence of a unique loop in the center of $\text{Poly}(S, \pi)$ surrounded by the outer base pairs of its symmetric slices. We call it the *central loop* of S , and denote it by \bigcirc^S . This central loop plays a crucial role in validating our slicing and swapping strategy (Lemmas 20 and 21) and determining the exact upper bound (Lemma 23) of symmetric secondary structures need to be backtracked.

Lemma 18. *For any R -fold symmetric secondary structure S , there exists a single loop, that we call the central loop \circ^S , that is not contained in any of the R symmetric slices. If $R > 2$ then \circ^S is a multiloop, if $R = 2$ then \circ^S is either a multiloop, stack, or an internal loop.*

Proof. Using our construction in Lemma 16, let $G_k \in \mathcal{G}$ be any symmetric slice, and assume a local indexing from 1 to $\frac{N}{R}$ for the bases in the segment I_k . Let $\mathcal{N}_k = \{(m, n) \in G_k : \neg \exists (m', n') \in G_k \text{ such that } m' < m < n < n'\}$. Intuitively, \mathcal{N}_k contains all outer base pairs of G_k , we call \mathcal{N}_k the *nesting set* of G_k as it determines how G_k will geometrically look like (when staring at it from the centre of the pizza).

Intuitively, we construct a path P_k as the concatenation of a segment of covalent bonds from G_k , and then a base pair in \mathcal{N}_k , then more covalent bonds, then a base pair, and so on. Formally, let $d = |\mathcal{N}_k|$, then $P_k = \llbracket 1, m_1 \rrbracket \cdot (m_1, n_1) \cdot \llbracket n_1, m_2 \rrbracket \cdot (m_2, n_2) \dots (m_c, n_c) \cdot \llbracket n_c, \frac{N}{R} \rrbracket$. Note that $\llbracket 1, m_1 \rrbracket$ and $\llbracket n_c, \frac{N}{R} \rrbracket$ may be substrands of length zero. Using this construction, P_k must be a path, otherwise G_k will be a disconnected graph contradicting Lemma 16.

Now, we will construct this central loop \circ^S as follows: for simplicity of notation, let $\mathcal{C}_R^b = \{b, b_2, \dots, b_R\}$, then $\circ^S = b.P_1.b_2.P_2 \dots b_R.P_R$. If $R > 2$, \circ^S must be a multiloop, since a multiloop is defined by being bordered by > 2 base pairs (hydrogen bonds). If $R = 2$, \circ^S will be a multiloop if and only if $|\mathcal{N}_k| \geq 2$ (this implies there are $R|\mathcal{N}_k| = 2|\mathcal{N}_k| > 2$ base pairs bordering the central loop), otherwise \circ^S will be an internal loop or stack. \circ^S can not be external loop otherwise this will contradict the connectedness of S , nor can \circ^S be a bulge nor hairpin loop as either of these will contradict the symmetry of S . \square

Because of the crucial importance of multiloops for our strategy, we highlight the multiloop energy model that is used in the standard dynamic programming algorithms. The free energy of a multiloop has the following linear form [10]:

$$\Delta G^{\text{multi}} = \Delta G_{\text{init}}^{\text{multi}} + b\Delta G_{\text{bp}}^{\text{multi}} + n\Delta G_{\text{nt}}^{\text{multi}}. \quad (6)$$

Where, $\Delta G_{\text{init}}^{\text{multi}}$ is called the penalty for formation of the multiloop, $\Delta G_{\text{bp}}^{\text{multi}}$ is called the penalty for each of its b base pairs that border the interior of the multiloop, and $\Delta G_{\text{nt}}^{\text{multi}}$ is called the penalty for each of the n free bases inside the multiloop. For any R -fold symmetric secondary structure S , $b\Delta G_{\text{bp}}^{\text{multi}}$ and $n\Delta G_{\text{nt}}^{\text{multi}}$ are shared equally between the R symmetric slices of $\text{Poly}(S, \pi)$, hence R divides both b and n . So, we denote $\Delta G^{\text{multi}} = \Delta G_{\text{init}}^{\text{multi}} + R(\Delta G_{\triangleright S}^{\text{multi}})$, where $\Delta G_{\triangleright S}^{\text{multi}}$ is the energy contribution of each symmetric slice of $\text{Poly}(S, \pi)$ to the multiloop free energy, such that $\Delta G_{\triangleright S}^{\text{multi}} = \frac{b}{R}\Delta G_{\text{bp}}^{\text{multi}} + \frac{n}{R}\Delta G_{\text{nt}}^{\text{multi}}$.

Remark 19. For any connected unpseudoknotted secondary structure S of c strands, we use $\overline{\Delta G}(S)$ to denote the snMFE of S , in other words $\overline{\Delta G}(S) = \sum_{l \in S} \Delta G(l) + (c - 1)\Delta G^{\text{rassoc}}$. It is clear that $\overline{\Delta G}(S) \leq \Delta G(S)$, as the symmetry correction $k_B T \log R \geq 0$.

Intuitively, the following lemma lets us take two symmetric pizzas with the same admissible symmetric cut for which we merely now their snMFE (we don't know their true MFE), and swap a slice from one into the other to get a new asymmetric pizza whose true MFE lies between their snMFEs. The key intuition is that we transforming symmetric secondary structures into an asymmetric one.

Lemma 20. *[Free-energy sandwich theorem for two R -fold rotational symmetric structures] For any two distinct ($R \geq 3$)-fold rotationally symmetric secondary structures, S_i and S_j , of c strands, such that $R \geq 3$ and $\overline{\Delta G}(S_i) \leq \overline{\Delta G}(S_j)$ and S_i and S_j have the same R -admissible backbone cut \mathcal{C}_R^b , then there exists at least one asymmetric secondary structure S_k , such that $\overline{\Delta G}(S_i) \leq \Delta G(S_k) \leq \overline{\Delta G}(S_j)$.*

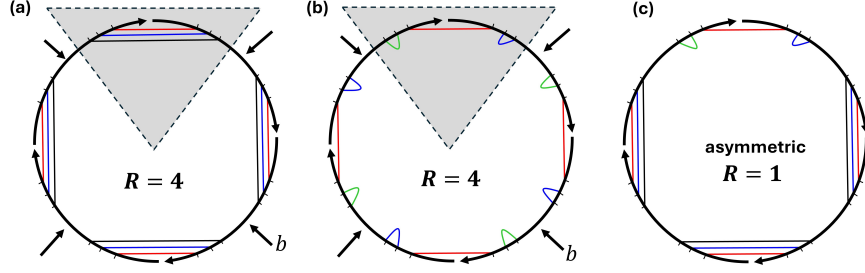


Figure 3: Slicing and swapping strategy for constructing new asymmetric structure by combining two symmetric structures with the same symmetric backbone cut. (a) 4-fold symmetric secondary structure S_i , with admissible 4-symmetric backbone cut \mathcal{C}_R^b . Black arrows: indicate the four covalent bonds forming \mathcal{C}_R^b generated by the covalent bond b . (b) 4-fold symmetric secondary structure S_j , sharing the same cut \mathcal{C}_R^b as S_i . Black arrows: indicate the four covalent bonds forming \mathcal{C}_R^b . (c) Asymmetric secondary structure S_k that is constructed by replacing the grey shaded ‘slice’ from S_i by its corresponding slice from S_j , using the proof of Lemma 20.

$\overline{\Delta G}(S_j)$. Furthermore, the statement holds if $R = 2$ and at least one of the central loops $\bigcirc^{S_i}, \bigcirc^{S_j}$ is a multiloop.

Proof. If $R \geq 3$, from Lemma 18, there exist two unique central multiloops for S_i and S_j , denoted by \bigcirc^{S_i} and \bigcirc^{S_j} . Also, if $R = 2$, by hypothesis, \bigcirc^{S_i} and \bigcirc^{S_j} are multiloops. We prove the claim with two cases:

Case 1. $\overline{\Delta G}(S_i) = \overline{\Delta G}(S_j)$:

$$\sum_{l \in S_i} \Delta G(l) + (c-1)\Delta G^{\text{assoc}} = \sum_{l \in S_j} \Delta G(l) + (c-1)\Delta G^{\text{assoc}} \quad (7)$$

$$\sum_{l \in S_i} \Delta G(l) = \sum_{l \in S_j} \Delta G(l) \quad (8)$$

$$R(\Delta G(\triangleright^{S_i})) + \Delta G(\bigcirc^{S_i}) = R(\Delta G(\triangleright^{S_j})) + \Delta G(\bigcirc^{S_j}) \quad (9)$$

$$R(\Delta G(\triangleright^{S_i})) + R\Delta G_{\triangleright^{S_i}}^{\text{multi}} + \Delta G_{\text{init}}^{\text{multi}} = R(\Delta G(\triangleright^{S_j})) + R\Delta G_{\triangleright^{S_j}}^{\text{multi}} + \Delta G_{\text{init}}^{\text{multi}} \quad (10)$$

$$R(\Delta G(\triangleright^{S_i}) + \Delta G_{\triangleright^{S_i}}^{\text{multi}}) = R(\Delta G(\triangleright^{S_j}) + \Delta G_{\triangleright^{S_j}}^{\text{multi}}) \quad (11)$$

$$\Delta G(\triangleright^{S_i}) + \Delta G_{\triangleright^{S_i}}^{\text{multi}} = \Delta G(\triangleright^{S_j}) + \Delta G_{\triangleright^{S_j}}^{\text{multi}} \quad (12)$$

We define a new secondary structure S_k using our slicing and swapping strategy, shown in Figure 3, by removing one slice from S_i , and adding its corresponding slice from S_j . Lemma 16 guarantees that the new secondary structure S_k is connected and unpsuedoknotted. Furthermore, S_k is asymmetric since $S_i \neq S_j$. S_k being asymmetric means that its rotational symmetry $R_k = 1$, $k_B T \log R_k = 0$ hence we can write:

$$\begin{aligned} \Delta G(S_k) &= (R-1) \left(\Delta G(\triangleright^{S_i}) + \Delta G_{\triangleright^{S_i}}^{\text{multi}} \right) + G_{\text{init}}^{\text{multi}} + (c-1)\Delta G^{\text{assoc}} + \left(\Delta G(\triangleright^{S_j}) + \Delta G_{\triangleright^{S_j}}^{\text{multi}} \right) \\ \Delta G(S_k) &= R \left(\Delta G(\triangleright^{S_i}) + \Delta G_{\triangleright^{S_i}}^{\text{multi}} \right) + \Delta G_{\text{init}}^{\text{multi}} + (c-1)\Delta G^{\text{assoc}} \end{aligned}$$

with the final step uses Eq. (12). Hence $\overline{\Delta G}(S_i) = \Delta G(S_k) = \overline{\Delta G}(S_j)$.

Case 2. $\overline{\Delta G}(S_i) < \overline{\Delta G}(S_j)$: Following the same algebraic manipulation as Eq. (7) to Eq. (12), but replacing $=$ with $<$, we get the following:

$$\Delta G(\triangleright^{S_i}) + \Delta G_{\triangleright^{S_i}}^{\text{multi}} < \Delta G(\triangleright^{S_j}) + \Delta G_{\triangleright^{S_j}}^{\text{multi}}$$

As before, we define a new connected asymmetric secondary structure S_k , using the same slicing and swapping strategy, resulting in: $\overline{\Delta G}(S_i) < \Delta G(S_k) < \overline{\Delta G}(S_j)$. □

Lemma 20 states that, if two symmetric secondary structures, having the same admissible R-symmetric backbone cut, belong to the same energy level based on symmetry-naive MFE algorithm, ignoring symmetry entropic correction, this implies the existence of at least one asymmetric secondary structure that actually belong to the same energy level because symmetry correction for asymmetric structures is zero. If the two secondary structures belong to two different energy levels, then there exist at least one asymmetric secondary structure that actually belong to an energy level strictly lies between the other two energy levels.

Intuition for the case of $R = 2$ and the central loop is not a multiloop. When $R = 2$, and the central loop is not a multiloop, the proof of Lemma 20 breaks. From Lemma 18, when $R = 2$ the central loop is either a multiloop, internal loop or stack loop. The multiloop case has been handled already (Lemma 20), and the stack loop case can be subsumed into the internal loop case, since stacks are considered a special type of internal loop in the standard energy model [10]. Instead of depending on having the same admissible 2-symmetric backbone cut, we depend on sharing the same central internal loop itself, this more restricted hypothesis implies having the same admissible 2-symmetric backbone cut too, allowing us to prove Lemma 21 using a similar strategy to Lemma 20.

Lemma 21. *[Free-energy sandwich theorem for two 2-fold rotational symmetric structures] For any two distinct 2-fold rotationally symmetric secondary structures, S_i and S_j , of c strands, such that $\overline{\Delta G}(S_i) \leq \overline{\Delta G}(S_j)$ and both have the same central internal loop $\bigcirc^{S_i} = \bigcirc^{S_j}$, then there exists at least one asymmetric secondary structure S_k , such that $\overline{\Delta G}(S_i) \leq \Delta G(S_k) \leq \overline{\Delta G}(S_j)$.*

Proof. Since $\bigcirc^{S_i} = \bigcirc^{S_j}$, then both have the same admissible 2-symmetric backbone cut as any covalent bond b that belong to any side of the internal loop can be its generator.

$$\begin{aligned} \overline{\Delta G}(S_i) &\leq \overline{\Delta G}(S_j) \\ \sum_{l \in S_i} \Delta G(l) + (c-1)\Delta G^{\text{assoc}} &\leq \sum_{l \in S_j} \Delta G(l) + (c-1)\Delta G^{\text{assoc}} \\ \sum_{l \in S_i} \Delta G(l) &\leq \sum_{l \in S_j} \Delta G(l) \\ 2(\Delta G(\triangleright^{S_i})) + \Delta G(\bigcirc^{S_i}) &\leq 2(\Delta G(\triangleright^{S_j})) + \Delta G(\bigcirc^{S_j}) \\ \Delta G(\triangleright^{S_i}) &\leq \Delta G(\triangleright^{S_j}) \end{aligned}$$

We define a new secondary structure S_k using our slicing and swapping strategy, shown in Figure 3, by removing one slice (half in this case) from S_i , and adding its corresponding slice from S_j . Note that S_k will have also the same central internal loop $\bigcirc^{S_k} = \bigcirc^{S_i}$. Lemma 16 guarantees that S_k is connected and unpsudoknotted. Since S_k is asymmetric:

$$\Delta G(S_k) = \Delta G(\triangleright^{S_i}) + \Delta G(\triangleright^{S_j}) + \Delta G(\bigcirc^{S_k}) + (c-1)\Delta G^{\text{assoc}}$$

Which implies that $\overline{\Delta G}(S_i) \leq \Delta G(S_k) \leq \overline{\Delta G}(S_j)$. □

We now have two sandwich theorems that we can use to construct an asymmetric structure: Lemmas 20 and 21. In Section 4 we give a backtracking algorithm to search for suitable S_i and S_j , with the goal of applying either one of these two sandwich theorems to S_i and S_j . To get an overall polynomial bound for the backtracking algorithm, we wish to bound, given S_i , how many secondary structures to scan before finding a suitable S_j . Lemma 13 gives this upper bound on this number when applying Lemma 20. Next, Lemma 22 gives this upper bound when applying Lemma 21.

Unfortunately, the bound in Lemma 22 is larger than Lemma 13, since the energy model is more complex for internal loops than multiloops [11].

Lemma 22 (Upper bound on number of central internal loops). *For any set of c strands with specific ordering π , for any set \mathcal{T} of 2-fold rotational symmetric secondary structures ($R = 2$), such that each has a distinct internal central loop, the cardinality of \mathcal{T} , $|\mathcal{T}| \leq \sum_{s \in y} (\|A\|_s \|T\|_s + \|G\|_s \|C\|_s) \leq N^2/16$, where y is a fundamental component of π , such that $\pi = y^2$, and $\|B\|_s$ denotes the number of bases in strand s of type B for all $B \in \{A, T, G, C\}$.*

Proof. Let \mathcal{T} be any set of 2-fold rotational symmetric secondary structures. Since each $S \in \mathcal{T}$ has a distinct internal central loop, we focus only on giving an upper bound on the maximum number of distinct internal central loops. Since $R = 2$, the two base pairs forming any central internal loop must be within two strands of the same type X of the same order m within their fundamental components (for example the strands are X_m^1 and X_m^2), otherwise we have a disconnected secondary structure due to the existence of nicks.

Only one of the two base pairs of any internal central loop needs to be specified explicitly, since, by symmetry, the other base pair is automatically determined. So, by considering all base pairs (including many that are irrelevant), the number of all distinct central internal loops is $\leq \sum_{s \in y} (\|A\|_s \|T\|_s + \|G\|_s \|C\|_s)$. Hence, $|\mathcal{T}| \leq \sum_{s \in y} (\|A\|_s \|T\|_s + \|G\|_s \|C\|_s)$. Using the two following number theoretic facts:

- If we have two indistinguishable strands, of the same type, X , of length n , the maximum intra-base pairs between them happens when the sequence of X is a word over $\{A, T\}$ or $\{G, C\}$ such that $\|A\|_X = \lfloor \frac{n}{2} \rfloor$ and $\|T\|_X = \lceil \frac{n}{2} \rceil$ or vice versa, and the same for $\{G, T\}$.
- For any integer $n > 0$, if $n = n_1 + n_2 + \dots + n_k$, such that $n_i \geq 0$ for all $i \in \{1, 2, \dots, k\}$, then $n^2 \geq n_1^2 + n_2^2 + \dots + n_k^2$.

We get the following:

$$\begin{aligned} \sum_{s \in y} (\|A\|_s \|T\|_s + \|G\|_s \|C\|_s) &\leq \left\lceil \frac{|s_1|}{2} \right\rceil \left\lfloor \frac{|s_1|}{2} \right\rfloor + \left\lceil \frac{|s_2|}{2} \right\rceil \left\lfloor \frac{|s_2|}{2} \right\rfloor + \dots + \left\lceil \frac{|s_{c/2}|}{2} \right\rceil \left\lfloor \frac{|s_{c/2}|}{2} \right\rfloor \\ &\leq \left(\frac{|s_1|}{2} \right)^2 + \left(\frac{|s_2|}{2} \right)^2 + \dots + \left(\frac{|s_{c/2}|}{2} \right)^2 \\ &= \frac{|s_1|^2 + |s_2|^2 + \dots + |s_{c/2}|^2}{4} \\ &\leq \frac{(N/2)^2}{4} = \frac{N^2}{16} \end{aligned}$$

where $s_i, i \in \{1, \dots, c\}$, are strand types. Hence: $|\mathcal{T}| \leq \sum_{s \in y} (\|A\|_s \|T\|_s + \|G\|_s \|C\|_s) \leq N^2/16$. \square

3.3 Polynomial upper bound on number of symmetric secondary structures (for future backtracking)

Lemma 23. *Given an ordering π of c strands, for any set \mathcal{T} of distinct symmetric secondary structures such that*

1. *for any two ($R > 2$)-fold symmetric secondary structures $S_i, S_j \in \mathcal{T}$, where S_i and S_j have different admissible R -symmetric backbone cuts (we mean all possible cuts are different), and*
2. *for any two 2-fold symmetric secondary structures $S_i, S_j \in \mathcal{T}$, where S_i and S_j have different admissible R -symmetric backbone cuts (all possible cuts are different) or different central internal loops,*

then $|\mathcal{T}| \leq \mathcal{U}$, where $\mathcal{U} = \frac{N-c}{v(\pi)} [\sigma(v(\pi)) - v(\pi)] + \frac{N^2}{16} = \mathcal{O}(N^2)$.

Proof. The proof is a trivial implication of Lemmas 13 and 22. (More formally: Let $\mathcal{U} = \mathcal{U}_1 + \mathcal{U}_2$ where \mathcal{U}_1 is the upper bound on the number of unique symmetric backbone cuts (Lemma 13), and \mathcal{U}_2 is the upper bound on the number of unique central internal loops (Lemma 22). Assume for the sake of contradiction that $|\mathcal{T}| > \mathcal{U}$. From the pigeon hole principle, $|\mathcal{T}| > \mathcal{U}$ implies repeating at least one symmetric backbone cut or a central internal loop contradicting the hypothesis about structures of \mathcal{T} .) \square

The (bad) quadratic bound in Lemma 22 is not that frequent: In particular, that bound only appears when $R = 2$ and the central loop is an internal loop for both symmetric secondary structures (since $R = 2$ this implies that the repetition number for every strand type is *even*, which in practice, say, for random or typical systems, may not be frequent). In particular the following lemma gives a *linear* bound when the repetition number of at least one strand type is odd.

Lemma 24. *For any R -fold rotationally symmetric secondary structure S , with ordering π , such that R is even, then the repetition number of each strand type must be even. Hence for any system of c strands (k strand types) such that the repetition number of some strand type is odd, then \mathcal{U} , where $\mathcal{U} = \frac{N-c}{v(\pi)} [\sigma(v(\pi)) - v(\pi)] = \mathcal{O}(N)$.*

Proof. Suppose S is a R -fold rotational symmetric such that R is even. From Lemma 34, R divides $v(\pi)$, which implies $v(\pi)$ is even too. Since $\pi = x^{v(\pi)}$ then $\pi = y^2$ such that $y = x^{v(\pi)/2}$, and this is valid only if the repetition number of each strand type is even. The linearity of \mathcal{U} follows directly if repetition number of at least one strand type is odd. \square

4 Backtracking to find the true MFE

In this section, we give a backtracking procedure, Algorithm 2 in Appendix C, to give our main result (Theorem 1). First, we run our augmentation of the known symmetry-naive MFE (sn-MFE) algorithm—Algorithm 1 in Appendix B, which returns some matrices which are input to the backtracking algorithm, Algorithm 2. Our multistranded backtracking algorithm builds on the single-stranded backtracking algorithm of Wuchty et al. [45], which in turn follows Waterman and Byers [40], although we make several technical modifications. In particular, distinctions with that previous work [45, 40] include:

1. We generalise backtracking from single-stranded to multistranded, which has a slightly different MFE algorithm, consistent with Dirks et al and Fornace et al [10, 15] (i.e. as implemented by the NUPACK software); in particular to ensure the connectedness of secondary structures (a non-issue for [45, 40]).

2. We make major changes to the core of the backtracking algorithm to ensure generation of all secondary structures, at each of a specified number of energy levels, in energy level order (which is different from the Wuchty et al’s [45] approach of backtracking all sub-optimal secondary structures that lie between the snMFE and any arbitrary upper limit above it).
3. We extend the refinement cases of Wuchty et al [45] to handle our auxiliary matrices in such a way that yields a good running time.

4.1 Partially and fully specified structures

Definition 25 (Partially and fully specified structure \mathcal{S}). A partially specified structure $\mathcal{S} = (\delta, \mathcal{P}, E_{L_S})$, where δ is a stack of disjoint segments of one or more DNA strands $\{[i, j]^t.[k, l]^{t'} \dots\}$ where $[i, j]^t$ is the top of the stack, such that i and j are the end bases of the segment $[i, j]$, $t \in \{\square, b, m\}$ is the type of each segment, such that $t = \square$ means the existence of a base pair between i and j , is as yet undetermined, $t = b$ means there is a base pair between i and j , and $t = m$ means that entire segment $[i, j]$ is part of a multiloop. \mathcal{P} is a set of base pairs formed in \mathcal{S} , and E_{L_S} is the energy of all loops that are ‘completely formed’ in \mathcal{S} . If $\delta = \phi$, we call \mathcal{S} a fully specified structure.

A fully specified structure is a connected unpseudoknotted secondary structure. For any segment $[i, j]^t$, label t is assigned according to how a segment is generated through *refinement* from another segment, formalized in Section 4.2, label t is needed in switching the backtracking between the appropriate matrices of the snMFE algorithm. We will denote the minimum free energy attainable from segment $[i, j]^t$, by $E([i, j]^t)$, which we get directly from the appropriate matrix $M, M^b, M^m, M^{b:int}, M^{b:mul},$ or $M^{m:2}$, that are returned by the snMFE algorithm (Algorithm 1), based on t , full details are in Appendix B. The domain of the function E is extended to include the set of all partially specified structures, in addition to the set of all segments, $\mathcal{S} = (\delta, \mathcal{P}, E_{L_S})$ so that E gives the minimum free energy attainable from \mathcal{S} , respecting the refinement rules formalized in Section 4.2, as follows:

$$E(\mathcal{S}) = E_{L_S} + \sum_{[m, n]^t \in \delta} E([m, n]^t) \quad (13)$$

Any partially specified structure $\mathcal{S} = (\delta, \mathcal{P}, E_{L_S})$ represents a set of all structures that have the base pairs \mathcal{P} in common: we can think of \mathcal{S} as the root of the tree of these structures, all intermediate nodes of this tree will be partially specified structures, and its leaves will be fully specified structures, and $E(\mathcal{S})$ is the minimum free energy attainable from this tree where all its nodes, structures, are further *refinements* of \mathcal{S} .

Definition 26 (Refinement of a partially specified structure). A structure $\mathcal{S}' = (\delta', \mathcal{P}', E_{L_{S'}})$ is called a refinement of the partially specified structure $\mathcal{S} = (\delta, \mathcal{P}, E_{L_S})$ if $\mathcal{P} \subseteq \mathcal{P}'$, and for each segment $[i', j']^{t'} \in \delta'$ there exist a segment $[i, j]^t \in \delta$ such that $[i', j']^{t'} \subseteq [i, j]^t$.

4.2 Analysis of the backtracking algorithm refinement rules

The backtracking algorithm starts with $\mathcal{S} = ([1, N]^\square, \phi, 0)$, which represents the whole system of strands with a specific strand order, π , without any base pair formed, $\mathcal{P} = \phi$, hence no loops are formed too, $E_{L_S} = 0$. \mathcal{S} is the parent node of the tree of any possible structure. Now, we will outline the main refinement procedure of the generic partial structure $\mathcal{S} = ([i, j]^t, \delta, \mathcal{P}, E_{L_S})$ that has been chosen, at the beginning of each iteration of the backtracking algorithm (Algorithm 2), from some array \mathcal{R}_z , the array of partially specified structures associated with each secondary

structure $S_z \in \{S_1, \dots, S_{\mathcal{U}}\}$, which is the secondary structure number z , of the worst case \mathcal{U} secondary structures we need to scan (Lemma 23), such that S_z is completely scanned during the backtracking. The segment $I = [i, j]^t$, the top of the segments stack of \mathcal{S} , will be popped and refined based on the type of label t resulting in a new refined structure \mathcal{S}' . Matrices M , M^b , M^m , and the new auxiliary matrices $M^{b:\text{int}}$, $M^{b:\text{mul}}$, and $M^{m:2}$, returned by Algorithm 1, will be used to compute the minimum free energy $E(\mathcal{S}')$ attainable from the refined partially specified structure \mathcal{S}' .

Given that the algorithm scans, or backtracks, all secondary structures in energy level \mathcal{E} , and \mathcal{B} is the best candidate for the true MFE at the moment, then the *acceptance criteria* of any refined partially specified structure \mathcal{S}' is:

$$E(\mathcal{S}') \leq \mathcal{B} \quad (14)$$

This acceptance criteria is checked after each refinement case, and if it is satisfied, \mathcal{S}' will be added on the array of partially specified structures \mathcal{R}_u , for some $u \in \{1, \dots, \mathcal{U}\}$, for further refinements in future, where \mathcal{R}_u is the secondary structure currently being scanned. Note that, because of the strict sequential scanning of the backtracking algorithm (Remark 30), the acceptance criteria implicitly implies that $\mathcal{E} \leq E(\mathcal{S}')$. Also, the acceptance criteria guarantees the connectedness of at least one potential fully specified structure which is a child of \mathcal{S}' (in Algorithm 2, setting $E(\mathcal{S}') = +\infty$ implies a disconnected or invalid structure).

There are 3 cases based on the type of t of the segment $I = [i, j]^t$ that has been popped (as mentioned above) from the stack δ :

1. $t = \square$ (recall, \square means: the existence of a base pair between i and j is undetermined):

In this case we backtrack in matrix M .

i and j are the end bases of I , and the possible refinements, based on Eq. (1) in Figure 4, are:

- Subcase: If the base j , at the $3'$ end of the segment $[i, j]$, is unpaired, that will result in the new partial structure (i.e. excluding j and moving to $j - 1$):

$$\mathcal{S}' = ([i, j - 1]^\square, \delta, \mathcal{P}, E_{L_S}) \text{ such that } E(\mathcal{S}') = M_{i, j-1} + E_{L_S} + \sum_{[m, n]^t \in \delta} E([m, n]^t).$$

- Subcase: If the base j forms a base pair with base $d \in [i, j - 1]$, we need to scan all such $d \in [i, j - 1]$, and for each we have the new partial structure:

$$\mathcal{S}' = ([i, d - 1]^\square, [d, j]^b, \delta, \mathcal{P}, E_{L_S}) \text{ such that } E(\mathcal{S}') = M_{i, d-1} + M_{d, j}^b + E_{L_S} + \sum_{[m, n]^t \in \delta} E([m, n]^t).$$

Note that we did not add the base pair (d, j) to \mathcal{P} at this step, but we shall do when refining the interval $[d, j]^b$ enclosed by (d, j) [45].

Then the acceptance criteria will be checked after each of the two sub-cases above. The backtracking algorithm have to check up to $\mathcal{O}(N)$ refined structures (because of d spans $\leq N$ bases in subcase 2), and hence save up to $\mathcal{O}(N)$ refined structures to \mathcal{R}_u in the worst case.

2. Case $t = b$ (recall: a base pair is formed between the end bases i and j of $[i, j]^b$ segment):

In this case we backtrack in matrix M^b . Now, assume the segment $[i, j]^b$ is popped from the stack δ , based on Eq. (2) in Figure 4, there are four subcases:

- **Hairpin loop** formation: If (i, j) is closing a hairpin loop (Figure 4(b)), this will result in the new partial structure:

$$\mathcal{S}' = (\delta, \mathcal{P} \cup \{(i, j)\}, E_{L_S} + \Delta G_{i, j}^{\text{hairpin}}) \text{ such that } E(\mathcal{S}') = \Delta G_{i, j}^{\text{hairpin}} + E_{L_S} + \sum_{[m, n]^t \in \delta} E([m, n]^t).$$

- **Interior loop** formation: We need to scan all possible base pairs (d, e) that bind to form an interior loop along with (i, j) (Figure 4(b)). Scanning all pairs in a straightforward way would lead to checking up to $\mathcal{O}(N^2)$ refined structures, which would end up with a poor final worst-case time complexity of the backtracking algorithm. Instead, we scan these base pairs in a different way, that keeps the number of refined structures that we need to check at each iteration to $\mathcal{O}(N)$. We achieve this by introducing a new auxiliary matrix, called $M^{\text{b:int}}$, in the snMFE algorithm, Algorithm 1.

Modifying the generic form of segment I is essential, in this case, the new segment generic form will be $I = [i, j]_{\text{int}:k}^b$, such that $k \in [i + 1, j - 1]$, which means that any base $d \in [k, j - 1]$ is unpaired, hence not included in the second base pair formation to complete the interior loop with (i, j) . When a new segment $[i, j]^b$ is just generated as a refinement from another segment, $[i, j]^b$ will be interpreted inside this case as $[i, j]_{\text{int}:j}^b$, which means any base $d \in [i + 1, j - 1]$ can be part of the second base pair closing the current interior loop. Given $I = [i, j]_{\text{int}:k}^b$, there are two cases:

- 1) If the base $k - 1$ is also unpaired, this will result in the new partial structure:

$$\mathcal{S}' = ([i, j]_{\text{int}:k-1}^b \cdot \delta, \mathcal{P}, E_{L_S}) \text{ such that } E(\mathcal{S}') = M_{i,j,k-2}^{\text{b:int}} + E_{L_S} + \sum_{[m,n]^t \in \delta} E([m, n]^t).$$

- 2) If the base $k - 1$ is paired with another base $d \in [i + 1, k - 2]$ closing the interior loop, this will result in the new partial structure:

$$\mathcal{S}' = ([d, k-1]^b \cdot \delta, \mathcal{P} \cup \{(i, j)\}, E_{L_S} + \Delta G_{i,d,k-1,j}^{\text{interior}}) \text{ such that } E(\mathcal{S}') = M_{d,k-1}^b + \Delta G_{i,d,k-1,j}^{\text{interior}} + E_{L_S} + \sum_{[m,n]^t \in \delta} E([m, n]^t).$$

- **Multiloop** formation: In this case we also need to scan all possible pairs (d, e) that will be used to form a multi-loop to the 3' end (Figure 4(b)), so we will follow the same strategy as the case of interior loop formation, by introducing another new auxiliary matrix, called $M^{\text{b:mul}}$, in the symmetry agnostic MFE algorithm, Algorithm 1. The generic form of I in this case will be updated to $I = [i, j]_{\text{mul}:k}^b$ such that $k \in [i + 1, j - 1]$, which means that any base $d \in [k, j - 1]$ is unpaired, hence not included in the forming any base pair inside this multiloop along with (i, j) . When a new segment $[i, j]^b$ is just generated as a refinement from another segment, $[i, j]^b$ will be interpreted inside this case as $[i, j]_{\text{mul}:j}^b$, which means any base $d \in [i + 1, j - 1]$ can be part of base pair formation inside this multiloop. Given $I = [i, j]_{\text{mul}:k}^b$, there are two cases:

- 1) If $k - 1$ is also unpaired, this will result in the new partial structure:

$$\mathcal{S}' = ([i, j]_{\text{mul}:k-1}^b \cdot \delta, \mathcal{P}, E_{L_S}) \text{ such that } E(\mathcal{S}') = M_{i,j,k-2}^{\text{b:mul}} + E_{L_S} + \sum_{[m,n]^t \in \delta} E([m, n]^t).$$

- 2) If the base $k - 1$ is paired with another base $d \in [i + 1, k - 2]$, this will result in the new partial structure:

$$\mathcal{S}' = ([i + 1, d-1]^m \cdot [d, k-1]^b \cdot \delta, \mathcal{P} \cup \{(i, j)\}, \Delta G_{\text{init}}^{\text{multi}} + 2\Delta G_{\text{bp}}^{\text{multi}} + (j - k)\Delta G_{\text{nt}}^{\text{multi}} + E_{L_S})$$

such that $E(\mathcal{S}') = M_{i+1,d-1}^m + M_{d,k-1}^b + \Delta G_{\text{init}}^{\text{multi}} + 2\Delta G_{\text{bp}}^{\text{multi}} + (j - k)\Delta G_{\text{nt}}^{\text{multi}} + E_{L_S} + \sum_{[m,n]^t \in \delta} E([m, n]^t).$

- **Exterior loop** formation: All bases $z \in [i, j]$ such that $[z, z + 1]$ is a nick (Figure 1, transition between two strands), are scanned (Figure 4(b)), leading to the new partial structure:

$$\mathcal{S}' = ([i + 1, z]^\square \cdot [z + 1, j - 1]^\square \cdot \delta, \mathcal{P} \cup \{(i, j)\}, E_{L_S}) \text{ such that } E(\mathcal{S}') = M_{i+1,z} + M_{z+1,j-1} + E_{L_S} + \sum_{[m,n]^t \in \delta} E([m, n]^t).$$

Then the acceptance criteria will be checked after each sub-case. Now, with the aid of the introduced new auxiliary matrices $M^{\text{b:int}}$ and $M^{\text{b:mul}}$, the backtracking algorithm checks up to $\mathcal{O}(N)$ refined structures, and hence saves up to $\mathcal{O}(N)$ refined structures to \mathcal{R}_u in the worst case. Without the new auxiliary matrices (in this case of $t = b$), the backtracking algorithm will check up to $\mathcal{O}(N^2)$ refined structures, and saves up to $\mathcal{O}(N^2)$ refined structures to \mathcal{R}_u .

3. Case $t = m$ (recall: the segment $[i, j]^m$ is a part of a multiloop):

We backtrack in matrix M^m . Now, assume the segment $[i, j]^m$ is popped from the stack, based on Eq. (3) in Figure 4, there are two subcases:

- If there exists exactly one additional base pair (d, e) defining the multiloop (Figure 4(c)), then we will scan for all possible pairs (d, e) that could be used. Following the same strategy of scanning introduced before (i.e. in case 2. $t = b$, interior loop or multiloop) to reduce time in interior and multiloop formation cases when $t = b$, there are two cases:

1) If j is unpaired, this will result in the new partial structure:

$$\mathcal{S}' = ([i, j - 1]^m, \delta, \mathcal{P}, E_{L_S} + \Delta G_{\text{nt}}^{\text{multi}}) \text{ such that } E(\mathcal{S}') = M_{i, j-1}^m + \Delta G_{\text{nt}}^{\text{multi}} + E_{L_S} + \sum_{[m, n]^t \in \delta} E([m, n]^t).$$

2) If the base j is paired with another base $d \in [i, j - 1]$ defining the multiloop, this will result in the new partial structure:

$$\mathcal{S}' = ([d, j]^b, \delta, \mathcal{P}, E_{L_S} + \Delta G_{\text{bp}}^{\text{multi}} + (d - i)\Delta G_{\text{nt}}^{\text{multi}}) \text{ such that } E(\mathcal{S}') = M_{d, j}^b + \Delta G_{\text{bp}}^{\text{multi}} + (d - i)\Delta G_{\text{nt}}^{\text{multi}} + E_{L_S} + \sum_{[m, n]^t \in \delta} E([m, n]^t).$$

- If there exist more than one base pair defining the multiloop, all possible pairs (d, e) are scanned (Figure 4(c)). Following the same strategy of scanning, and using one of the new auxiliary matrices, called $M^{\text{m:2}}$, in the snMFE algorithm, Algorithm 1.

The generic form of I in this case will be updated to $I = [i, j]_{\text{mul:k}}^m$ such that $k \in [i, j]$, which means that any base $d \in [k, j]$ is unpaired, hence not included in the forming of any base pair inside this multiloop. When a new segment $[i, j]^m$ is just generated as a refinement from another segment, $[i, j]^m$ will be interpreted inside this case as $[i, j]_{\text{mul:j-1}}^m$, which means any base $d \in [i, j]$ can be part of base pair formation inside this multiloop. Given $I = [i, j]_{\text{mul:k}}^m$, there are two cases:

1) If the base $k - 1$ is also unpaired, this will result in the new partial structure:

$$\mathcal{S}' = ([i, j]_{\text{mul:k-1}}^m, \delta, \mathcal{P}, E_{L_S}) \text{ such that } E(\mathcal{S}') = M_{i, j, k-2}^{\text{m:2}} + E_{L_S} + \sum_{[m, n]^t \in \delta} E([m, n]^t).$$

2) If the base $k - 1$ is paired with another base $d \in [i, k - 2]$, this will result in the new partial structure:

$$\mathcal{S}' = ([i, d - 1]^m, [d, k - 1]^b, \delta, \mathcal{P}, \Delta G_{\text{bp}}^{\text{multi}} + (j - k + 1)\Delta G_{\text{nt}}^{\text{multi}} + E_{L_S}) \text{ such that } E(\mathcal{S}') = M_{i, d-1}^m + M_{d, k-1}^b + \Delta G_{\text{bp}}^{\text{multi}} + (j - k + 1)\Delta G_{\text{nt}}^{\text{multi}} + E_{L_S} + \sum_{[m, n]^t \in \delta} E([m, n]^t).$$

Then the acceptance criteria will be checked after each sub-case. Now, with the aid of the introduced new auxiliary matrices $M^{\text{mul:2}}$, the backtracking algorithm checks up to $\mathcal{O}(N)$ refined structures, hence saves up to $\mathcal{O}(N)$ refined structures to \mathcal{R}_u , in the worst case.

Remark 27. For any \mathcal{S} and \mathcal{S}' such that \mathcal{S}' is a refinement of \mathcal{S} based on refinement rules described above, $E(\mathcal{S}) \leq E(\mathcal{S}')$. Also, note that the form of the new refined structure \mathcal{S}' in each case of refinement cases is different, and hence leads to a different fully specified structure which

guarantees that each secondary structure S_u encountered during the backtracking is scanned exactly once.

Remark 28. For all the cases above where \mathcal{S}' is refinement of \mathcal{S} , the stack δ and the base pairs set \mathcal{P} are parts (common) of each refined structure \mathcal{S}' , hence it is enough to save them once, which takes $\mathcal{O}(N)$ space, and for each refined structure \mathcal{S}' , we need to save only the additional base pairs (one base pair in the worst case, hence $\mathcal{O}(1)$ space), or the new segments (two segments in the worst case, hence $\mathcal{O}(1)$ space) that are pushed on the top of δ based on the refinement case. In total saving the all $\mathcal{O}(N)$ refined structures that are generated from all cases requires $\mathcal{O}(N)$ space.

Remark 29. For all the cases above where \mathcal{S}' is refinement of \mathcal{S} , $\mathcal{H} = E_{L\mathcal{S}} + \sum_{[m,n]^t \in \delta} E([m,n]^t)$ is repeatedly used to compute $E(\mathcal{S}')$ again and again, hence it is enough to compute it once, which takes only $\mathcal{O}(N)$ time. In total, if \mathcal{H} is pre-computed once in this way, computing $E(\mathcal{S}')$ takes $\mathcal{O}(1)$ time.

After scanning the secondary structure S_u completely, the partially specified structure $\mathcal{S}' \in \mathcal{R}_u$, such that $E(\mathcal{S}') = \min_{\mathcal{S} \in \mathcal{R}_u} \{E(\mathcal{S})\}$ will be computed and saved. And a new partially specified structure \mathcal{S} is chosen as follows:

$$\mathcal{S} = \min_{z \in \{1, \dots, u\}} \left\{ \min_{\mathcal{S}' \in \mathcal{R}_z} \{E(\mathcal{S}')\} \right\} \quad (15)$$

Where $\{S_1, \dots, S_u\}$ is the set of distinct secondary structures that are completely scanned until the moment, where $u < \mathcal{U}$. Then the minimum ($\min_{\mathcal{S}' \in \mathcal{R}_z} \{E(\mathcal{S}')\}$) of the array $\mathcal{R}_{z'}$ where \mathcal{S} is choose from, will be computed again and saved for future iterations.

Remark 30. Eq. (15) guarantees sequential scanning of the backtracking algorithm through energy levels without skipping any potential structure, due to free energy minimality. Also, note that for all $z \in \{1, \dots, u\}$, the $\min_{\mathcal{S}' \in \mathcal{R}_z} \{E(\mathcal{S}')\}$ is already computed and saved, as in each iteration we choose only the minimum over the set of all minimum energies of each array, so we lose only one the minimum of some array $\mathcal{R}_{z'}$, so $\mathcal{R}_{z'}$ is the only one we need to compute its minimum again in $\mathcal{O}(N^2)$ time.

The same refinement process starts again with that new selected partially specified structure \mathcal{S} . This backtracking procedure continues in this way until one of the three following conditions occurs first:

1. The algorithm scans an *asymmetric* secondary structure S_u , then the true MFE = $\Delta G(S_u)$, as a direct consequence of $\Delta G(S_u) \leq \mathcal{B}$, where we recall that \mathcal{B} was the best candidate value for true MFE, or
2. The algorithm exceeds the upper bound \mathcal{U} of the number of symmetric secondary structures to be scanned, then the true MFE = \mathcal{E} , the energy of the last scanned energy level which is also the snMFE of that last completely scanned symmetric secondary structure S_u , as a direct consequence of Lemmas 20, 21 and 23 (meaning we have two symmetric structures of snMFE equal to \mathcal{E} with the same admissible cut, hence we can make a new pizza: an asymmetric secondary structure of true MFE \mathcal{E}), or
3. The algorithm starts scanning a new energy level $\mathcal{E}' > \mathcal{B}$, then the true MFE = \mathcal{B} , as \mathcal{B} is the best candidate for the true MFE that we got from a previously scanned symmetric secondary structure.

Whichever of the three cases occurs, the true MFE is returned (and a secondary structure with that true MFE is constructed).

4.3 Time and space complexity analysis of the backtracking algorithm

The backtracking algorithm needs to scan up to $\mathcal{U} = \mathcal{O}(N^2)$ secondary structures in the worst case (Lemma 23), so the total time complexity of the backtracking algorithms is $\mathcal{O}(\mathcal{U}\mathcal{W})$, where \mathcal{W} is the time complexity of scanning only one secondary structure and setting up the scene for the next iteration by choosing the new partially specified structure required to scan the next secondary structure.

Analysis for scanning only one secondary structure in the backtracking algorithm. To scan (construct) one secondary structure S_u , we need in the worst case $N = \mathcal{O}(N)$ refinement steps, as each step either ignores a base or forms a base pair. We showed in our analysis, in Section 4.2, and based on $t \in \{\square, b, m\}$, that each step checks up to $\mathcal{O}(N)$ refined structures and saves up to $\mathcal{O}(N)$ refined structures to \mathcal{R}_u , the array of refined structures associated with S_u . In total, by Remark 29, scanning one secondary structure takes $\mathcal{O}(N^2)$, as \mathcal{R}_u contains $\mathcal{O}(N^2)$ structure, hence computing the minimum of \mathcal{R}_u takes $\mathcal{O}(N^2)$ time.

The last step is to see what is the time complexity of choosing the new partially specified structure \mathcal{S} for the next iteration based on Eq. (15), from Remark 30 this step takes $\mathcal{O}(N^2)$ time, as the minimum of all the $\mathcal{U} = \mathcal{O}(N^2)$ arrays is already computed and stored.

So, in total scanning one secondary structure and setting up the scene for the next iteration by choosing the new partially specified structure \mathcal{S} takes $\mathcal{O}(N^2)$ time.

Remark 28 shows that each array \mathcal{R}_u requires $\mathcal{O}(N^2)$ space, hence in total the backtracking algorithm requires $\mathcal{O}(N^4)$ space to store the all \mathcal{R}_u such that $u \in \{1, \dots, \mathcal{U}\}$. This analysis leads to the following result.

Lemma 31. *The running time of the backtracking algorithm, Algorithm 2 and Section 4.2, for a set of $c = \mathcal{O}(1)$ DNA or RNA strands of total length N bases, is $\mathcal{O}(N^4(c-1)!)$, and it requires $\mathcal{O}(N^4)$ space.*

Remark 32. We should note that, changing the strategy, used in Eq. (15), for choosing the new partially specified structure \mathcal{S} can help in reducing the space complexity of the backtracking algorithm from $\mathcal{O}(N^4)$ to $\mathcal{O}(N^3)$ (the same space complexity as snMFE Algorithm 1) with the trade off increasing the time complexity to be $\mathcal{O}(N^4 \log N(c-1)!)$ instead of $\mathcal{O}(N^4(c-1)!)$. As we know that we need to scan only $\mathcal{U} = \mathcal{O}(N^2)$ secondary structures, so we do not need to store all elements of arrays \mathcal{R}_z where $z \in \{1, \dots, u\}$. Only the minimum \mathcal{U} candidates should be stored. By sorting \mathcal{R}_u , the array of partially specified structures that we obtain after constructing the secondary structure S_u (the secondary structure number u , of the worst case \mathcal{U}). \mathcal{R}_u can be sorted in $\mathcal{O}(N^2 \log N)$ time then merged in $\mathcal{O}(N^2)$ time with the already sorted array, that we obtain cumulatively through time from the previous iterations.

As we noted before in Lemma 24, that the (bad) quadratic upper bound \mathcal{U} in Lemma 22 is very restricted and rare, and for systems of c strands (k strand types) where the repetition number of some strand type is odd, Lemma 24 shows that the upper bound \mathcal{U} is linear. Hence, the time complexity of the backtracking algorithm is $\mathcal{O}(N^3(c-1)!)$ and it requires $\mathcal{O}(N^3)$ space.

5 Time and space analysis of MFE algorithm

Theorem 1. *There is an $\mathcal{O}(N^4(c-1)!)$ time and $\mathcal{O}(N^4)$ space algorithm for the Minimum Free Energy unpseudoknotted secondary structure prediction problem, including rotational symmetry, for a set of $c = \mathcal{O}(1)$ DNA or RNA strands of total length N bases.*

Proof. Dirks et al’s snMFE algorithm runs in time $\mathcal{O}(N^4(c-1)!)$ and space $\mathcal{O}(N^2)$ [10]. In Algorithm 1, we give their snMFE pseudocode but augmented with three matrices $M^{\text{b:int}}$, $M^{\text{b:mul}}$, and $M^{\text{m:2}}$, with no asymptotic change to run time but an increase to $\mathcal{O}(N^3)$ space. Also, by Lemma 31 the time complexity of our backtracking algorithm, Algorithm 2, is $\mathcal{O}(N^4(c-1)!)$, and the space complexity is $\mathcal{O}(N^4)$.

Hence after running both algorithms we get an $\mathcal{O}(N^4(c-1)!)$ algorithm for the MFE unpseudoknotted secondary structure prediction problem, including rotational symmetry, with $\mathcal{O}(N^4)$ as space complexity.

By Remark 32 we can get another alternative algorithm of $\mathcal{O}(N^4 \log N(c-1)!)$ time and $\mathcal{O}(N^3)$ space. \square

Acknowledgements

We thank Constantine Evans for his helpful comments on the statistical mechanics origin of the MFE rotational symmetry penalty, and Dave Doty for comments on the manuscript. Ahmed Shalaby would like to thank Dvořák for composing his masterpiece, Symphony No. 9 “From the New World”.

References

- [1] Tatsuya Akutsu. Dynamic programming algorithms for RNA secondary structure prediction with pseudoknots. *Discrete Applied Mathematics*, 104(1-3):45–62, 2000.
- [2] Peter William Atkins, Julio De Paula, and James Keeler. *Atkins’ physical chemistry*. Oxford university press, 2023.
- [3] Kimon Boehmer, Sarah J Berkemer, Sebastian Will, and Yann Ponty. Rna triplet repeats: Improved algorithms for structure prediction and interactions. 2024. 24th Workshop on Algorithms in Bioinformatics (WABI), to appear. URL: <https://hal.science/hal-04589903>.
- [4] Edward Bormashenko. Entropy, information, and symmetry: Ordered is symmetrical. *Entropy*, 22(1):11, 2019.
- [5] Richard A Brualdi. *Introductory combinatorics*. Pearson Education India, 1977.
- [6] Gourab Chatterjee, Neil Dalchau, Richard A. Muscat, Andrew Phillips, and Georg Seelig. A spatially localized architecture for fast and modular DNA computing. *Nature Nanotechnology*, 12(9):920–927, Sep 2017. doi:10.1038/nnano.2017.127.
- [7] Ho-Lin Chen, Anne Condon, and Hosna Jabbari. An $\mathcal{O}(n^5)$ algorithm for MFE prediction of kissing hairpins and 4-chains in nucleic acids. *Journal of Computational Biology*, 16(6):803–815, 2009.
- [8] Alexander Churkin, Matan Drory Retwitzer, Vladimir Reinharz, Yann Ponty, Jérôme Waldispühl, and Danny Barash. Design of RNAs: comparing programs for inverse RNA folding. *Briefings in bioinformatics*, 19(2):350–358, 2018.
- [9] Anne Condon, Monir Hajiaghayi, and Chris Thachuk. Predicting minimum free energy structures of multi-stranded nucleic acid complexes is APX-hard. In *27th International Conference on DNA Computing and Molecular Programming (DNA 27)*. Schloss Dagstuhl-Leibniz-Zentrum für Informatik, 2021.

- [10] Robert M Dirks, Justin S Bois, Joseph M Schaeffer, Erik Winfree, and Niles A Pierce. Thermodynamic analysis of interacting nucleic acid strands. *SIAM review*, 49(1):65–88, 2007.
- [11] Robert M Dirks and Niles A Pierce. A partition function algorithm for nucleic acid secondary structure including pseudoknots. *Journal of computational chemistry*, 24(13):1664–1677, 2003.
- [12] Robert M Dirks and Niles A Pierce. An algorithm for computing nucleic acid base-pairing probabilities including pseudoknots. *Journal of computational chemistry*, 25(10):1295–1304, 2004.
- [13] David Doty and Benjamin Lee. nuad: Nucleic acid designer, March 2022. Uses, and generalises, sequence design principles from [44]. URL: <https://github.com/UC-Davis-molecular-computing/nuad>.
- [14] Joshua Fern and Rebecca Schulman. Design and characterization of dna strand-displacement circuits in serum-supplemented cell medium. *ACS Synthetic Biology*, 6(9):1774–1783, 2017. doi:10.1021/acssynbio.7b00105.
- [15] Mark E Fornace, Nicholas J Porubsky, and Niles A Pierce. A unified dynamic programming framework for the analysis of interacting nucleic acid strands: enhanced models, scalability, and speed. *ACS Synthetic Biology*, 9(10):2665–2678, 2020.
- [16] Cody Geary, Paul WK Rothmund, and Ebbe S Andersen. A single-stranded architecture for cotranscriptional folding of RNA nanostructures. *Science*, 345(6198):799–804, 2014.
- [17] Ivo L Hofacker, Christian M Reidys, and Peter F Stadler. Symmetric circular matchings and RNA folding. *Discrete mathematics*, 312(1):100–112, 2012.
- [18] Hosna Jabbari, Ian Wark, Carlo Montemagno, and Sebastian Will. Knotty: efficient and accurate prediction of complex RNA pseudoknot structures. *Bioinformatics*, 34(22):3849–3856, 2018.
- [19] Ronny Lorenz, Stephan H Bernhart, Christian Höner zu Siederdisen, Hakim Tafer, Christoph Flamm, Peter F Stadler, and Ivo L Hofacker. ViennaRNA package 2.0. *Algorithms for molecular biology*, 6:1–14, 2011.
- [20] Rune B Lyngsø and Christian NS Pedersen. Pseudoknots in RNA secondary structures. In *Proceedings of the fourth annual international conference on Computational molecular biology*, pages 201–209, 2000.
- [21] Rune B Lyngsø and Christian NS Pedersen. RNA pseudoknot prediction in energy-based models. *Journal of computational biology*, 7(3-4):409–427, 2000.
- [22] Rune B Lyngsø, Michael Zuker, and CN Pedersen. Fast evaluation of internal loops in RNA secondary structure prediction. *Bioinformatics (Oxford, England)*, 15(6):440–445, 1999.
- [23] David H Mathews, Jeffrey Sabina, Michael Zuker, and Douglas H Turner. Expanded sequence dependence of thermodynamic parameters improves prediction of RNA secondary structure. *Journal of molecular biology*, 288(5):911–940, 1999.
- [24] John S McCaskill. The equilibrium partition function and base pair binding probabilities for RNA secondary structure. *Biopolymers: Original Research on Biomolecules*, 29(6-7):1105–1119, 1990.

- [25] W Keith Nicholson. *Introduction to abstract algebra*. John Wiley & Sons, 2012.
- [26] Ruth Nussinov and Ann B Jacobson. Fast algorithm for predicting the secondary structure of single-stranded RNA. *Proceedings of the National Academy of Sciences*, 77(11):6309–6313, 1980.
- [27] Ruth Nussinov, George Pieczenik, Jerrold R Griggs, and Daniel J Kleitman. Algorithms for loop matchings. *SIAM Journal on Applied mathematics*, 35(1):68–82, 1978.
- [28] Lulu Qian and Erik Winfree. Scaling up digital circuit computation with DNA strand displacement cascades. *Science*, 332(6034):1196–1201, 2011.
- [29] Jens Reeder and Robert Giegerich. Design, implementation and evaluation of a practical pseudoknot folding algorithm based on thermodynamics. *BMC bioinformatics*, 5:1–12, 2004.
- [30] Elena Rivas and Sean R Eddy. A dynamic programming algorithm for RNA structure prediction including pseudoknots. *Journal of molecular biology*, 285(5):2053–2068, 1999.
- [31] John SantaLucia Jr. A unified view of polymer, dumbbell, and oligonucleotide DNA nearest-neighbor thermodynamics. *Proceedings of the National Academy of Sciences*, 95(4):1460–1465, 1998.
- [32] John SantaLucia Jr and Donald Hicks. The thermodynamics of DNA structural motifs. *Annu. Rev. Biophys. Biomol. Struct.*, 33:415–440, 2004.
- [33] Joe Sawada. A fast algorithm to generate necklaces with fixed content. *Theoretical Computer Science*, 301(1-3):477–489, 2003.
- [34] Georg Seelig, David Soloveichik, David Yu Zhang, and Erik Winfree. Enzyme-free nucleic acid logic circuits. *science*, 314(5805):1585–1588, 2006.
- [35] Robert J Silbey, Robert A Alberty, George A Papadantonakis, and Mounqi G Bawendi. *Physical chemistry*. John Wiley & Sons, 2022.
- [36] Anupama J. Thubagere, Wei Li, Robert F. Johnson, Zibo Chen, Shayan Doroudi, Yae Lim Lee, Gregory Izatt, Sarah Wittman, Niranjan Srinivas, Damien Woods, Erik Winfree, and Lulu Qian. A cargo-sorting DNA robot. *Science*, 357(6356), 2017.
- [37] Ignacio Tinoco, Olke C Uhlenbeck, and Mark D Levine. Estimation of secondary structure in ribonucleic acids. *Nature*, 230(5293):362–367, 1971.
- [38] Yasuo Uemura, Aki Hasegawa, Satoshi Kobayashi, and Takashi Yokomori. Tree adjoining grammars for RNA structure prediction. *Theoretical computer science*, 210(2):277–303, 1999.
- [39] Boya Wang, Siyuan Stella Wang, Cameron Chalk, Andrew D Ellington, and David Soloveichik. Parallel molecular computation on digital data stored in DNA. *Proceedings of the National Academy of Sciences*, 120(37):e2217330120, 2023.
- [40] Michael S Waterman and Thomas H Byers. A dynamic programming algorithm to find all solutions in a neighborhood of the optimum. *Mathematical Biosciences*, 77(1-2):179–188, 1985.
- [41] Michael S Waterman and Temple F Smith. Rapid dynamic programming algorithms for RNA secondary structure. *Advances in Applied Mathematics*, 7(4):455–464, 1986.

- [42] Douglas Brent West et al. *Introduction to graph theory*, volume 2. Prentice hall Upper Saddle River, 2001.
- [43] Sungwook Woo and Paul WK Rothemund. Programmable molecular recognition based on the geometry of DNA nanostructures. *Nature chemistry*, 3(8):620, 2011.
- [44] Damien Woods, David Doty, Cameron Myhrvold, Joy Hui, Felix Zhou, Peng Yin, and Erik Winfree. Diverse and robust molecular algorithms using reprogrammable DNA self-assembly. *Nature*, 567(7748):366–372, 2019.
- [45] Stefan Wuchty, Walter Fontana, Ivo L Hofacker, and Peter Schuster. Complete suboptimal folding of RNA and the stability of secondary structures. *Biopolymers: Original Research on Biomolecules*, 49(2):145–165, 1999.
- [46] David Yu Zhang and Georg Seelig. Dynamic DNA nanotechnology using strand-displacement reactions. *Nature chemistry*, 3(2):103–113, 2011.
- [47] Michael Zuker. Mfold web server for nucleic acid folding and hybridization prediction. *Nucleic acids research*, 31(13):3406–3415, 2003.
- [48] Michael Zuker and David Sankoff. RNA secondary structures and their prediction. *Bulletin of mathematical biology*, 46:591–621, 1984.
- [49] Michael Zuker and Patrick Stiegler. Optimal computer folding of large RNA sequences using thermodynamics and auxiliary information. *Nucleic acids research*, 9(1):133–148, 1981.

A Appendix: Useful lemmas

Lemma 33 (factors of π). *For any nonempty circular permutation π and any prefix y of π that is not its fundamental component x , such that $|y| > |x|$, if $\pi = y^n$ then $|x|$ divides $|y|$.*

Proof. Suppose for contradiction that such y and n exist, so $x^{v(\pi)} = y^n$ which means that $v(\pi)|x| = n|y|$. As $|x|$ does not divide $|y|$, from division algorithm we can write $|y| = a|x| + b$ for some remainder $0 < b < |x|$.

Suppose the infinite string W that is just an infinite repeat of π and hence an infinite repeat of x and y . Let's suppose a simple function $f(i)$ that return the character at index i of W , as $\pi = x^{v(\pi)} = y^n$ that means that $f(i) = f(i + \alpha|x|) = f(i + \beta|y|)$ for any α and β . Then $f(i) = f(i + a\beta|x| + \beta b)$. For $\beta = 1$ that implies that $f(i) = f(i + b)$, which implies the existence of a smaller repeating prefix of π since $b < |x|$ which contradicts the fact that x is the fundamental component of π . \square

The following lemma restricts us to deal with only specific and constant number of different folding rotational symmetries, and hence constant different symmetry corrections in total.

Lemma 34. *If S is R -fold rotational symmetric secondary structure, with a specific circular permutation π , then R must be a divisor of $v(\pi)$.*

Proof. As $R = |H|$ a subgroup of G^π , and from Lagrange theorem for finite groups [25], which says that for any finite group G , the order of every subgroup of G divides the order of G . So, R divides $|G^\pi| = v(\pi)$. Also, from the fundamental theorem of cyclic groups, as we know that H is a subgroup of the cyclic group G^π , then $H = \langle \rho^d \rangle$ for some $\rho^d \in G^\pi$, H is generated by ρ^d . Hence, H is the *unique* subgroup of order $|H| = v(\pi)/d$. \square

Lemma 35. *For any connected unpseudoknotted secondary structure S , if there exists at least one base pair (i, j) such that $\llbracket i, j \rrbracket > \frac{N}{R}$, then S can not be R -fold rotationally symmetric.*

Proof. For all $R > 2$, suppose for the sake of contradiction that S is R -fold rotational symmetric secondary structure and such base pair (i, j) exists, from symmetry this implies the existence of another $(R - 1)$ different base pairs each with same segment length as $\llbracket i, j \rrbracket$, so the total length of the system must be higher than number of bases N , so at least two base pairs must intersect forming a pseudoknot, which contradicts the fact that S is pseudoknot-free.

For $R = 2$, suppose such base pair (i, j) exists, then this can only happen if (i, j) is a central base pair, a diameter in $\text{Poly}(S, \pi)$, such that $\llbracket i, j \rrbracket = \frac{N}{2} + 1 > \frac{N}{2}$. This is impossible as the symmetry implies that i and j are of the same type, that there exists a base which is complement to itself. \square

B Appendix: Symmetry-naive MFE (snMFE) algorithm

Algorithm 1, shown in Figure 4, computes snMFE for a constant number, $c = \mathcal{O}(1)$, of interacting nucleic acid strands. We should note that: Algorithm 1 is a straightforward conversion of the partition function algorithm from Dirks et al. [10]. Algorithm 1 ignores rotational symmetry, if the predicted snMFE structure from this algorithm happens to be asymmetric, then the output of Algorithm 1 is the true MFE as there is no symmetry correction penalty for asymmetric secondary structures. However, if the snMFE structure is an R -fold symmetric secondary structure, then its free energy must be corrected by $+k_B T \log R$, a positive value, then it is not guaranteed that the snMFE will be the true MFE without scanning all secondary structures in the window of $k_B T \log R$ above snMFE, and applying any needed symmetry corrections to the free energy of each secondary structure that lies in that window. Wuchty et al. [45] showed that this window of secondary structures could scale exponentially with N , which shows why this strategy fails. But in this work, we proved that only a polynomial number of these structures are enough for predicting the true MFE.

We introduced new three-dimensional matrices $M^{b:\text{int}}$, $M^{b:\text{mul}}$, $M^{m:2}$ to help in reducing the time complexity of the backtracking algorithm. For any segment $[i, j]^b$, if $i + 2 \leq k \leq j - 1$, $M_{i,j,k}^{b:\text{int}}$ will contain the minimum free energy attainable from the segment $[i, j]^b$ such that all bases d , such that $k < d < j$ are unpaired, and there exist exactly one base pair (m, n) , such that $i + 1 \leq m < n \leq k$, (i, j) and (m, n) are forming together an internal loop. The same for $M_{i,j,k}^{b:\text{mul}}$, except that there exist more than one base pair (m, n) , such that $i + 1 \leq m < n \leq k$, forming together a multiloop with (i, j) .

For any segment $[i, j]^m$, if $i + 1 \leq k \leq j$, $M_{i,j,k}^{m:2}$ contains the minimum free energy attainable from the segment $[i, j]^m$ such that all bases d , such that $k < d \leq j$ are unpaired, and there exist more than one base pair (m, n) , such that $i \leq m < n \leq k$, forming together a multiloop with (i, j) .

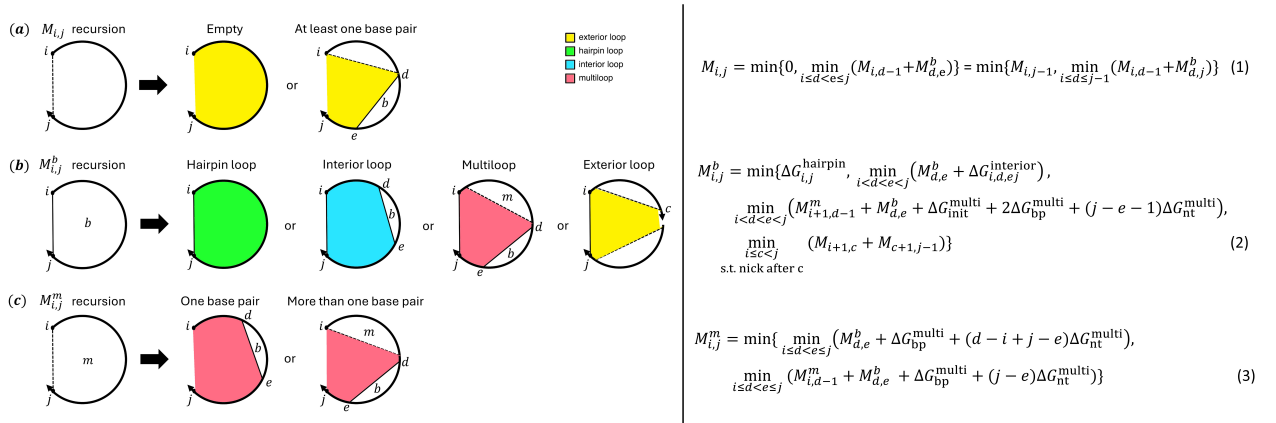


Figure 4: snMFE dynamic program recursion diagrams (left) and recursion equations (right). A solid straight line indicates a base pair and a dashed line demarcates a region without implying that the connected bases are paired. Shaded regions correspond to loop free energies that are explicitly incorporated at the current level of recursion. See [11, 15] for full details.

Algorithm 1 Symmetry-naive MFE (snMFE) algorithm pseudocode that takes as input: $c = \mathcal{O}(1)$ strands with total number of bases (length) N and strand ordering π . Runs in $\mathcal{O}(N^4)$ time and $\mathcal{O}(N^3)$ space with recursive calls illustrated in Figure 4. Nicks between strands are denoted by half indices (e.g. $x + \frac{1}{2}$). The function $\eta[i + \frac{1}{2}, j + \frac{1}{2}]$ returns the number of nicks in the interval $[i + \frac{1}{2}, j + \frac{1}{2}]$. The shorthand $\eta[i + \frac{1}{2}]$ is equivalent to $\eta[i + \frac{1}{2}, i + \frac{1}{2}]$ and by convention, $\eta[i + \frac{1}{2}, i - \frac{1}{2}] = 0$.

```

1: Initialize  $M, M^b, M^m, M^{b:int}, M^{b:mul}, M^{m:2}$  by setting all values to  $+\infty$ , except  $M_{i,i-1} = 0$  for all  $i = 1, \dots, N$ 
2: for  $l \leftarrow 1 \dots N$  do
3:   for  $i \leftarrow 1 \dots N - l + 1$  do
4:      $j = i + l - 1$ 
5:     if  $\eta[i + \frac{1}{2}, j - \frac{1}{2}] == 0$  then  $M_{i,j}^b = \Delta G_{i,j}^{hairpin}$  ▷  $M^b$  recursion equations
6:     end if ▷ hairpin loop requires no nicks
7:      $\min_{int}^b = \min_{mul}^b = \min_{mul}^m = +\infty$ 
8:     for  $e \leftarrow i + 2 \dots j - 1$  do ▷ loop over all possible 3'-most pairs  $(d, e)$ 
9:       for  $d \leftarrow i + 1 \dots e - 1$  do
10:        if  $\eta[i + \frac{1}{2}, d - \frac{1}{2}] == 0$  and  $\eta[e + \frac{1}{2}, j - \frac{1}{2}] == 0$  then  $M_{i,j}^b = \min\{M_{i,j}^b, M_{d,e}^b + \Delta G_{i,d,e,j}^{interior}\}$ 
11:          if  $(M_{d,e}^b + \Delta G_{i,d,e,j}^{interior}) < \min_{int}^b$  then  $\min_{int}^b = M_{d,e}^b + \Delta G_{i,d,e,j}^{interior}$ 
12:          end if
13:          end if
14:          if  $\eta[e + \frac{1}{2}, j - \frac{1}{2}] == 0$  and  $\eta[i + \frac{1}{2}] == 0$  and  $\eta[d - \frac{1}{2}] == 0$  then ▷ multiloop: no nicks
15:             $M_{i,j}^b = \min\{M_{i,j}^b, M_{d,e}^b + M_{i+1,d-1}^m + \Delta G_{init}^{multi} + 2\Delta G_{bp}^{multi} + (j - e - 1)\Delta G_{nt}^{multi}\}$ 
16:            if  $(M_{i+1,d-1}^m + M_{d,e}^b + \Delta G_{init}^{multi} + 2\Delta G_{bp}^{multi} + (j - e - 1)\Delta G_{nt}^{multi}) < \min_{mul}^b$  then
17:               $\min_{mul}^b = M_{i+1,d-1}^m + M_{d,e}^b + \Delta G_{init}^{multi} + 2\Delta G_{bp}^{multi} + (j - e - 1)\Delta G_{nt}^{multi}$ 
18:            end if
19:          end if
20:        end for
21:         $M_{i,j,e}^{b:int} = \min_{int}^b; M_{i,j,e}^{b:mul} = \min_{mul}^b$  ▷ for the new auxiliary matrices
22:      end for
23:      for  $x \in \{i, \dots, j + 1\}$  s.t.  $\eta[x + \frac{1}{2}] = 1$  do ▷ loop over all nicks  $\in [i + \frac{1}{2}, j - \frac{1}{2}]$ 
24:        if  $(\eta[i + \frac{1}{2}] == 0$  and  $\eta[j - \frac{1}{2}] == 0)$  or  $(i == j - 1)$  or  $(x == i$  and  $\eta[j - \frac{1}{2}] == 0)$  or
25:           $(x == j - 1$  and  $\eta[i + \frac{1}{2}] == 0)$  then
26:             $M_{i,j}^b = \min\{M_{i,j}^b, M_{i+1,x} + M_{x+1,j-1}\}$  ▷ exterior loops
27:          end if
28:        end for
29:        if  $\eta[i + \frac{1}{2}, j - \frac{1}{2}] == 0$  then  $M_{i,j} = 0$  ▷  $M, M^m$  recursion equations
30:        end if ▷ empty substructure
31:        for  $e \leftarrow i + 1 \dots j$  do ▷ loop over all possible 3'-most pairs  $(d, e)$ 
32:          for  $d \leftarrow i \dots e - 1$  do
33:            if  $\eta[e + \frac{1}{2}, j - \frac{1}{2}] == 0$  then
34:              if  $\eta[d - \frac{1}{2}] == 0$  or  $d == i$  then  $M_{i,j} = \min\{M_{i,j}, M_{i,d-1} + M_{d,e}\}$ 
35:              end if
36:              if  $\eta[i + \frac{1}{2}, d - \frac{1}{2}] == 0$  then
37:                 $M_{i,j}^m = \min\{M_{i,j}^m, M_{d,e}^b + \Delta G_{bp}^{multi} + (d - i + j - e)\Delta G_{nt}^{multi}\}$  ▷ single base pair
38:              end if
39:              if  $\eta[d - \frac{1}{2}] == 0$  then
40:                 $M_{i,j}^m = \min\{M_{i,j}^m, M_{d,e}^b + M_{i,d-1}^m + \Delta G_{bp}^{multi} + (j - e)\Delta G_{nt}^{multi}\}$  ▷ more than one base pair
41:                if  $(M_{i,d-1}^m + M_{d,e}^b + \Delta G_{bp}^{multi} + (j - e)\Delta G_{nt}^{multi}) < \min_{mul}^m$  then
42:                   $\min_{mul}^m = M_{i,d-1}^m + M_{d,e}^b + \Delta G_{bp}^{multi} + (j - e)\Delta G_{nt}^{multi}$ 
43:                end if
44:              end if
45:            end if
46:          end for
47:           $M_{i,j,e}^{m:2} = \min_{mul}^m$ 
48:        end for
49:      end for
50:    end for ▷ next line returns the snMFE for ordering  $\pi$ , and several matrices for future backtracking
51:  return  $M_{1,N} + (c - 1)\Delta G^{assoc}$ ; and matrices:  $M, M^b, M^m, M^{b:int}, M^{b:mul}, M^{m:2}$ 

```

C Appendix: Backtracking algorithm to find the true MFE

In this backtracking algorithm, we use $[i, j]_{q:k}^t$ to denote the generic form of segment that has been popped from the stack δ , where $t \in \{\square, b, m\}$, and $q \in \{\text{mul}, \text{int}, \text{null}\}$, where null means (nothing), and $k \in [i, j]$. For the full details, see Section 4.2.

Algorithm 2 Backtracking pseudocode that takes as input: $c = \mathcal{O}(1)$ strands with total number of bases (length) N and strand ordering π . Runs in $\mathcal{O}(N^4)$ time and $\mathcal{O}(N^4)$ space, and assumes there are $k \leq c$ strand types given as a *multiset*, each with an associated repetition number $n_1, \dots, n_k \in \mathbb{N}$, such that $n_1 + \dots + n_k = c$, with total length N . $[i, j]^t \leftarrow \delta$ denotes popping an element from stack δ , which is a segment, and assigning it to the generic segment $[i, j]^t$. And $\mathcal{S} \Rightarrow \mathcal{R}$ denotes pushing structure \mathcal{S} onto stack \mathcal{R} , and $E(\mathcal{S})$ is defined in Eq. (13), and all refinement cases are analyzed in Section 4.2.

```

1: if  $(n_1, n_2, \dots, n_k)$  are all even then                                 $\triangleright$  use Lemma 24 to set symmetric structure upperbound  $\mathcal{U}$ 
2:    $\mathcal{U} = \frac{N-c}{v(\pi)} [\sigma(v(\pi)) - v(\pi)] + \frac{N^2}{16}$                                  $\triangleright$  in  $\mathcal{O}(1)$  time
3: else
4:    $\mathcal{U} = \frac{N-c}{v(\pi)} [\sigma(v(\pi)) - v(\pi)]$ 
5: end if
6:  $\mathcal{E} = \text{snMFE}$                                                                  $\triangleright$  snMFE is returned by Algorithm 1
7:  $\mathcal{B} = \mathcal{E} + k_{\text{B}}T \log v(\pi)$                                                  $\triangleright$  where  $v(\pi)$  is the highest symmetry degree for the  $c$ -strands ordering  $\pi$ 
8:  $\mathcal{S} = ([1, N]^{\square}, \phi, 0)$                                                  $\triangleright$  the initial system (the parent of any possible structure)
9:  $(\delta, \mathcal{P}, E_{L_{\mathcal{S}}}) = \mathcal{S}$ 
10:  $u = 1$                                                                      $\triangleright$   $u$  is a symmetric secondary structures counter
11: while  $(u \leq \mathcal{U})$  do
12:    $y = \text{False}; w = \text{False}$                                                  $\triangleright$   $y$  and  $w$  are indicator variables
13:    $[i, j]_{q,k}^t \leftarrow \delta$ 
14:    $\mathcal{H} = E_{L_{\mathcal{S}}} + \sum_{[m,n]^t \in \delta} E([m, n]^t)$                                  $\triangleright$  in  $\mathcal{O}(N)$ , Remark 29
15:    $\mathcal{S} = (\delta, \mathcal{P}, E_{L_{\mathcal{S}}})$                                                  $\triangleright$  if all cases were not satisfied (just pop  $[i, j]_{q,k}^t$ )
16:   if  $(t == \square)$  then                                                     $\triangleright$  backtrack in matrix  $M$ 
17:      $\mathcal{S}' = ([i, j-1]^{\square}, \delta, \mathcal{P}, E_{L_{\mathcal{S}}})$                                  $\triangleright$  base  $j$  is not paired
18:      $E(\mathcal{S}') = M_{i,j-1} + \mathcal{H}$ 
19:     if  $(E(\mathcal{S}') \leq \mathcal{B})$  then
20:       if  $(y == \text{False} \text{ and } E(\mathcal{S}') == \mathcal{E})$  then
21:          $\mathcal{S} = \mathcal{S}'; y = \text{True}$ 
22:       else
23:          $\mathcal{S}' \Rightarrow \mathcal{R}_u$ 
24:       end if
25:     end if
26:     for  $d \in [i, j-1]$  do                                                 $\triangleright$  base  $j$  is paired with some base  $d$ 
27:        $\mathcal{S}' = ([i, d-1]^{\square}, [d, j]^b, \delta, \mathcal{P}, E_{L_{\mathcal{S}}})$ 
28:        $E(\mathcal{S}') = M_{i,d-1} + M_{d,j}^b + \mathcal{H}$ 
29:       if  $(M_{i,d-1} + M_{d,j}^b + \mathcal{H} \leq \mathcal{B})$  then
30:         if  $(y == F \text{ and } E(\mathcal{S}') == \mathcal{E})$  then
31:            $\mathcal{S} = \mathcal{S}'; y = T$ 
32:         else
33:            $\mathcal{S}' \Rightarrow \mathcal{R}_u$ 
34:         end if
35:       end if
36:     end for
37:   else if  $(t == b)$  then                                                 $\triangleright$  backtrack in matrix  $M^b$ 
38:     if  $(q == \text{null})$  then                                                 $\triangleright$  hairpin loop formation
39:        $\mathcal{S}' = (\delta, \mathcal{P} \cup \{(i, j)\}, E_{L_{\mathcal{S}}} + \Delta G_{i,j}^{\text{hairpin}})$ 
40:        $E(\mathcal{S}') = \Delta G_{i,j}^{\text{hairpin}} + \mathcal{H}$ 
41:       if  $(E(\mathcal{S}') \leq \mathcal{B})$  then
42:         if  $(y == F \text{ and } E(\mathcal{S}') == \mathcal{E})$  then
43:            $\mathcal{S} = \mathcal{S}'; y = T$ 
44:         else
45:            $\mathcal{S}' \Rightarrow \mathcal{R}_u$ 
46:         end if
47:       end if
48:     end if

```

Part 2 of backtracking algorithm

```

49:   if ( $q == \text{null}$ ) then  $\triangleright$  interpreting the segment to be in a valid form for internal loop case Section 4.2
50:      $q = \text{int}; k = j, w = \text{True}$ 
51:   end if
52:   if ( $q == \text{int}$ ) then
53:      $S' = ([i, j]_{\text{int}:k-1}^b, \delta, \mathcal{P}, E_{L_S})$   $\triangleright$  internal loop formation: base  $k - 1$  is unpaired
54:      $E(S') = M_{i,j,k-2}^{\text{b:int}} + \mathcal{H}$ 
55:     if ( $E(S') \leq \mathcal{B}$ ) then
56:       if ( $y == F$  and  $E(S') == \mathcal{E}$ ) then
57:          $S = S'; y = T$ 
58:       else  $S' \Rightarrow \mathcal{R}_u$ 
59:       end if
60:     end if
61:   end if
62:   if ( $w == \text{True}$ ) then
63:      $q = \text{null}; k = \text{null}, w = \text{False}$ 
64:   end if
65:   if ( $q == \text{null}$ ) then  $\triangleright$  internal loop formation: base  $k - 1$  is paired
66:     for  $d \in [i + 1, k - 2]$  do
67:        $S' = ([d, k - 1]^b, \delta, \mathcal{P} \cup \{(i, j)\}, E_{L_S} + \Delta G_{i,d,k-1,j}^{\text{interior}})$ 
68:        $E(S') = M_{d,k-1}^b + \Delta G_{i,d,k-1,j}^{\text{interior}} + \mathcal{H}$ 
69:       if ( $E(S') \leq \mathcal{B}$ ) then
70:         if ( $y == F$  and  $E(S') == \mathcal{E}$ ) then
71:            $S = S'; y = T$ 
72:         else  $S' \Rightarrow \mathcal{R}_u$ 
73:         end if
74:       end if
75:     end for
76:   end if
77:   if ( $q == \text{null}$ ) then  $\triangleright$  interpreting the segment to be in a valid form for multiloop case Section 4.2
78:      $q = \text{mul}; k = j, w = \text{True}$ 
79:   end if
80:   if ( $q == \text{mul}$ ) then
81:      $S' = ([i, j]_{\text{mul}:k-1}^b, \delta, \mathcal{P}, E_{L_S})$   $\triangleright$  multiloop formation: base  $k - 1$  is unpaired
82:      $E(S') = M_{i,j,k-2}^{\text{b:mul}} + \mathcal{H}$ 
83:     if ( $E(S') \leq \mathcal{B}$ ) then
84:       if ( $y == F$  and  $E(S') == \mathcal{E}$ ) then
85:          $S = S'; y = T$ 
86:       else
87:          $S' \Rightarrow \mathcal{R}_u$ 
88:       end if
89:     end if
90:   end if
91:   if ( $w == \text{True}$ ) then
92:      $q = \text{null}; k = \text{null}, w = \text{False}$ 
93:   end if
94:   if ( $q == \text{null}$ ) then  $\triangleright$  multiloop formation: base  $k - 1$  is paired
95:     for  $d \in [i + 1, k - 2]$  do
96:        $S' = ([i + 1, d - 1]^m, [d, k - 1]^b, \delta, \mathcal{P} \cup \{(i, j)\}, \Delta G_{\text{init}}^{\text{multi}} + 2\Delta G_{\text{bp}}^{\text{multi}} + (j - k)\Delta G_{\text{nt}}^{\text{multi}} + E_{L_S})$ 
97:        $E(S') = M_{i+1,d-1}^m + M_{d,k-1}^b + \Delta G_{\text{init}}^{\text{multi}} + 2\Delta G_{\text{bp}}^{\text{multi}} + (j - k)\Delta G_{\text{nt}}^{\text{multi}} + \mathcal{H}$ 
98:       if ( $E(S') \leq \mathcal{B}$ ) then
99:         if ( $y == F$  and  $E(S') == \mathcal{E}$ ) then
100:            $S = S'; y = T$ 
101:         else
102:            $S' \Rightarrow \mathcal{R}_u$ 
103:         end if
104:       end if
105:     end for
106:   end if

```

Part 3 of backtracking algorithm

```

107:   if ( $q == \text{null}$ ) then ▷ exterior loop formation
108:     for  $z \in [i, j]$  s.t.  $\eta[z + \frac{1}{2}] == 1$  do
109:        $S' = ([i + 1, z]^\square.[z + 1, j - 1]^\square.\delta, \mathcal{P} \cup \{(i, j)\}, E_{L_S})$ 
110:        $E(S') = M_{i+1,z} + M_{z+1,j-1} + \mathcal{H}$ 
111:       if ( $E(S') \leq \mathcal{B}$ ) then
112:         if ( $y == F$  and  $E(S') == \mathcal{E}$ ) then
113:            $S = S'; \quad y = T$ 
114:         else
115:            $S' \Rightarrow \mathcal{R}_u$ 
116:         end if
117:       end if
118:     end for
119:   end if
120: else if ( $t == m$ ) then ▷ backtrack in matrix  $M^m$ 
121:   if ( $q == \text{null}$ ) then ▷ multiloop case 1: base  $j$  is unpaired
122:      $S' = ([i, j - 1]^m.\delta, \mathcal{P}, E_{L_S} + \Delta G_{\text{nt}}^{\text{multi}})$ 
123:      $E(S') = M_{i,j-1}^m + \Delta G_{\text{nt}}^{\text{multi}} + \mathcal{H}$ 
124:     if ( $E(S') \leq \mathcal{B}$ ) then
125:       if ( $y == F$  and  $E(S') == \mathcal{E}$ ) then
126:          $S = S'; \quad y = T$ 
127:       else
128:          $S' \Rightarrow \mathcal{R}_u$ 
129:       end if
130:     end if
131:   end if
132: if ( $q == \text{null}$ ) then ▷ base  $j$  is paired
133:   for  $d \in [i, j - 1]$  do
134:      $S' = ([d, j]^b.\delta, \mathcal{P}, E_{L_S} + \Delta G_{\text{bp}}^{\text{multi}} + (d - i)\Delta G_{\text{nt}}^{\text{multi}})$ 
135:      $E(S') = M_{d,j}^b + \Delta G_{\text{bp}}^{\text{multi}} + (d - i)\Delta G_{\text{nt}}^{\text{multi}} + \mathcal{H}$ 
136:     if ( $E(S') \leq \mathcal{B}$ ) then
137:       if ( $y == F$  and  $E(S') == \mathcal{E}$ ) then
138:          $S = S'; \quad y = T$ 
139:       else
140:          $S' \Rightarrow \mathcal{R}_u$ 
141:       end if
142:     end if
143:   end for
144: end if
145: if ( $q == \text{null}$ ) then ▷ interpreting the segment to be in a valid form for multiloop case Section 4.2
146:    $q = \text{mul}; \quad k = j - 1, \quad w = \text{True}$ 
147: end if
148: if ( $q == \text{mul}$ ) then ▷ multiloop case 2: base  $k$  is unpaired
149:    $S' = ([i, j]_{\text{mul};k-1}^m.\delta, \mathcal{P}, E_{L_S})$ 
150:    $E(S') = M_{i,j,k-2}^{m;2} + \mathcal{H}$ 
151:   if ( $E(S') \leq \mathcal{B}$ ) then
152:     if ( $y == F$  and  $E(S') == \mathcal{E}$ ) then
153:        $S = S'; \quad y = T$ 
154:     else
155:        $S' \Rightarrow \mathcal{R}_u$ 
156:     end if
157:   end if
158: end if
159: if ( $w == \text{True}$ ) then
160:    $q = \text{null}; \quad k = \text{null}, \quad w = \text{False}$ 
161: end if

```

Part 4 of backtracking algorithm

```

162:     if ( $q == \text{null}$ ) then                                     ▷ base  $k - 1$  is paired
163:         for  $d \in [i, k - 2]$  do
164:              $S' = ([i, d - 1]^m \cdot [d, k - 1]^b \cdot \delta, \mathcal{P}, \Delta G_{\text{bp}}^{\text{multi}} + (j - k + 1)\Delta G_{\text{nt}}^{\text{multi}} + E_{L_S})$ 
165:              $E(S') = M_{i,d-1}^m + M_{d,k-1}^b + \Delta G_{\text{bp}}^{\text{multi}} + (j - k + 1)\Delta G_{\text{nt}}^{\text{multi}} + \mathcal{H}$ 
166:             if ( $E(S') \leq \mathcal{B}$ ) then
167:                 if ( $y == F$  and  $E(S') == \mathcal{E}$ ) then
168:                      $S = S'; \quad y = T$ 
169:                 else
170:                      $S' \Rightarrow \mathcal{R}_u$ 
171:                 end if
172:             end if
173:         end for
174:     end if
175: end if
176:  $(\delta, \mathcal{P}, E_{L_S}) = \mathcal{S}$ 
177: if ( $\delta == \phi$ ) then                                           ▷ scanning  $\mathcal{S}$  is done,  $\mathcal{S}$  is a fully specified structure
178:     Output secondary structure  $\mathcal{S}$  using its base pairs set  $\mathcal{P}$ 
179:     if ( $\mathcal{S}$  is asymmetric) then
180:         MFE =  $\Delta G(\mathcal{S})$                                        ▷  $\Delta G(\mathcal{S})$  is defined in Eq. (2), which also equals  $\mathcal{E}$  at the moment
181:         break                                                 ▷ break out of top-level while loop
182:     else
183:         Apply rot. symmetry correction to free energy of  $\mathcal{S}$  (i.e.  $\mathcal{E}' := \mathcal{E} + k_B T \log R$ ); if  $\mathcal{E}' < \mathcal{B}$  then  $\mathcal{B} := \mathcal{E}'$ 
184:          $\mathcal{S} = \min_{z \in \{1, \dots, u\}} \left\{ \min_{S' \in \mathcal{R}_z} \{E(S')\} \right\}$    ▷ Eq. (15), to ensure the sequential scanning over energy levels
185:          $u = u + 1$                                              ▷ increment symmetric secondary structures counter
186:          $(\delta, \mathcal{P}, E_{L_S}) = \mathcal{S}$ 
187:         if ( $E(\mathcal{S}) > \mathcal{B}$ ) then                               ▷ compare with the updated  $\mathcal{B}$ 
188:             MFE =  $\mathcal{B}$ 
189:             break                                             ▷ break out of top-level while loop
190:         else
191:              $\mathcal{E} = E(\mathcal{S})$ 
192:             MFE =  $\mathcal{E}$                                          ▷ in case the upper bound  $\mathcal{U}$  is exceeded
193:         end if
194:     end if
195: end if
196: end while
197: return MFE                                                     ▷ return the true MFE

```
